Localisation and expression of aquaporin-4 around arterioles, venules and capillaries in the rat spinal cord

By
Thomas Cusick
(41480848)

Australian School of Advanced Medicine

A thesis submitted for the partial fulfilment of the requirements for the degree of Master of Research in Neuroscience

Supervisor

Professor Marcus Stoodley

Australian School of Advanced Medicine, Faculty of Human Sciences, Macquarie University, Sydney, NSW, Australia

Key words: aquaporin-4, spinal cord, arterioles, venules, capillaries, immunohistochemistry

Abstract character count: 238

Word count:10,428

Number of figures: 18

Contents

Abstract

The traditional view of cerebrospinal fluid (CSF) circulation within the central nervous system (CNS) is that CSF is produced within the choroid plexus, flows slowly through the subarachnoid space (SAS), and is reabsorbed by arachnoid villi or around spinal nerves. Despite acceptance of this viewpoint, the mechanism by which CSF is moved around the CNS is not fully understood. Our current understanding of CSF flow within the brain is that fluid inflow occurs predominantly around peri-arterial spaces, whilst outflow occurs around peri-venular spaces. This fluid movement is believed to be mediated by the protein aquaporin-4 (AQP4). Whether AQP4 contributes to the movement of CSF within the spinal cord remains to be determined. The aim of the following study was to assess AQP4 expression in the rodent spinal cord in relation to microvasculature structures. Multiple labelling immunohistochemistry was performed on 6 and 12 week old rats to distinguish arterioles from venules, and capillaries were identified by measuring the diameter of each stained vessel. AQP4 was found around both arterioles and venules within the rodent spinal cord, and was expressed in higher levels in the younger rats. No overall difference was found between AQP4 expression levels around arterioles, venules and capillaries, however, expression of AQP4 was found to decrease as the diameter of arterioles increased. The results of this study lay the foundation for future experiments to assess the effect of AQP4 antagonism on fluid flow within the spinal cord.

Conflict of interest statement

The research in the following experiment was conducted in the absence of any commercial or financial relationships that could be construed as a potential conflict of interest.

Declaration of originality

I certify that the work in this thesis entitled “Localisation and expression of aquaporin-4 around arterioles, venules and capillaries in the rat spinal cord” has not previously been submitted for a degree nor has it been submitted as part of requirements for a degree to any other university or institution other than Macquarie University.

I also certify that the thesis is an original piece of research and it has been written by me. Any help and assistance that I have received in my research work and the preparation of the thesis itself have been appropriately acknowledged.

In addition, I certify that all information sources and literature used are indicated in the thesis.

The research presented in this thesis was approved by Macquarie University Ethics Review Committee, reference number: 2013/047-5 on 14 August 2014

Thomas Cusick

41480848

10/10/2014

Localisation and expression of aquaporin-4 around arterioles, venules and capillaries in the rat spinal cord

Cerebrospinal fluid (CSF) is a colourless fluid that surrounds the central nervous system (CNS) and physically supports the weight of the brain, protects brain tissue following impact, and functions as an intra-cerebral transport medium for nutrients, neuroendocrine substances and neurotransmitters (Nilsson et al., 1992;Stover et al., 1997). The daily volume of CSF produced in adult humans is approximately 500 – 600 ml (Johanson et al., 2008); ependymal cells of the choroid plexus are associated with more than two-thirds of this production, with the remainder generated in extra-choroidal sources such as the surface of the ventricles and the linings surrounding subarachnoid space (Craven, 2010). The traditional model of CSF movement within the CNS presumes that following production within the choroid plexus, CSF circulates from the lateral ventricles into the third and fourth ventricles; where it then leaves via median and lateral aperture to enter the subarachnoid space (Craven, 2010). Upon reaching the subarachnoid space, CSF travels around the spinal cord and brain until it is reabsorbed into venous sinuses by arachnoid villi and veins around cranial and spinal nerves (Chikly and Quaghebeur, 2013).

In contrast, the flow and regulation of CSF within the CNS is far more complex and dynamic than the widely accepted traditional model indicates. In order for efficient neuronal processing to occur within the CNS, extracellular fluid needs to be controlled in a stable microenvironment that is separate from the changeable environment of blood (Redzic, 2011). This is achieved by the presence of three distinct barrier layers: the blood-brain barrier, formed by capillary endothelial cells that separate circulating blood from brain interstitial fluid, the blood-CSF barrier, consisting of endothelial cells that separate CSF from the interstitial fluid of the choroid plexus, and lastly the arachnoid barrier which envelopes the brain (Laterra, 1999;Abbott, 2004;Redzic, 2011). Together, these barriers provide ionic homeostasis, prevent diffusion between brain fluids and blood, and provide transport processes for essential nutrients, ions and metabolic products (Abbott, 2004;Redzic, 2011).

Whilst the traditional model of CSF flow describes a straightforward pathway of how CSF is produced and reabsorbed, the mechanism that governs CSF movement throughout the CNS is not fully understood (Killer et al., 2007). This can be attributed to the fact that invasive flow measurements can significantly alter the natural motion of this fluid, and non-invasive studies are somewhat limited in resolution and accuracy in most areas that are not defined by a predominant axis such as the superior region of spinal subarachnoid space (Gupta et al., 2010). Therefore, despite limitations, phase-contrast magnetic resonance imaging (MRI) is currently the most widely used technique employed to study the flow of CSF non-invasively (Enzmann and Pelc, 1992). Whilst bulk flow of CSF throughout the CNS is important for maintaining normal pressure and CSF turnover (Wagshul and Johnston, 2013), rapid transport of tracer out of the CSF compartments is difficult to explain based on bulk drainage rates alone (Rennels et al., 1985). The results of flow-sensitive MRI studies have demonstrated that the majority of CSF flow is pulsatile (Greitz, 1993;Battal et al., 2011), and movement of CSF is the result of pulsations related to the cardiac cycle of the choroid plexus, and the subarachnoid portion of the cerebral arteries (Barkhof et al., 1994). In order to maintain homeostasis, CSF is constantly reabsorbed so that only 100-160 mL is present within the CNS at any time (Johanson et al., 2008). Under normal conditions, approximately 90% of CSF reabsorption occurs at intracranial sites, with the remainder taking place at spinal sites (Cottrell and Young, 2010).

CSF circulation around the subarachnoid space is traditionally believed to be a slow process (Ichimura et al., 1991). However, radiolabelled tracer injections into the lateral ventricle have revealed that CSF circulation is rapid throughout the ventricular system and various subarachnoid velae and cisterns (Ghersi-Egea et al., 1996). Furthermore, injections of horseradish peroxidase into the cisterna magna have indicated rapid flow from the subarachnoid space into the spinal cord (Stoodley et al., 1996). Building upon the traditional model of CSF flow, research using tracers has demonstrated that CSF from the subarachnoid space flows through perivascular spaces into the brain, brainstem and spinal cord (Stoodley et al., 1996;Stoodley et al., 1997;Iliff et al., 2012). Perivascular spaces – sometimes referred to as Virchow-Robin spaces – are fluid filled canals that surround perforating arteries and veins in the parenchyma of the brain (Esiri and Gay, 1990). Since first being described by Virchow (1851) and Robin (1859), the importance of these structures has been a subject of debate for over 150 years (Groeschel et al., 2006), largely in part to associations with diseases such as Alzheimer's (Chen et al., 2011) and multiple sclerosis (Etemadifar et al., 2011).

The brain is a unique organ that despite its complex architecture and high metabolic activity, lacks a specialised structure or the conventional lymphatic vasculature required to clear extracellular proteins and excess fluid from the interstitium (Cserr et al., 1992;Iliff and Nedergaard, 2013). However, in a recent publication, by Iliff *et al.* (2012), evidence has suggested that the movement of CSF through perivascular spaces is not only a pathway for fluid flow, but also a process that helps to facilitate the clearance of interstitial solutes such as amyloid β; fulfilling a role similar to the lymphatic system in other organs. Following injection of fluorescent tracers into the cisterna magna of mice, in vivo two-photon microscopy and ex vivo laser scanning confocal microscopy revealed rapid tracer movement inward along peri-arterial spaces, across the surrounding astrocytic linings, and into the brain interstitial space. After an extended period of time, this tracer movement was observed around peri-venular spaces when it exited the brain through either the medial internal cerebral veins or the lateral-ventral caudal rhinal veins. Together, these findings suggest that in the brain fluid inflow predominantly occurs around peri-arterial spaces, and fluid outflow at peri-venular spaces.

Aquaporins are integral membrane proteins that function as channels to facilitate water movement across cell membranes (Takata et al., 2004). Aquaporin-4 (AQP4); the most abundant aquaporin protein located in the CNS (Verkman, 2009), is highly polarized to the membranes of astrocytes lining peri-arterial and peri-venular spaces. As approximately 99% of CSF volume is water (Bulat et al., 2008), this protein is thought to play an important role in rapid fluid movement throughout the CNS, specifically by providing low resistance transecullar pathways (Papadopoulos and Verkman, 2005). In order to examine this relationship, Iliff et al. (2012) compared the clearance of radiolabeled tracers between wild-type and AQP4 knockout mice, and found that movement of tracer into the brain parenchyma was significantly reduced in knockout mice; suggesting that AQP4 helps to mediate water flux and facilitate movement of CSF into and through the brain interstitium. The movement of CSF from the subarachnoid space into the brain by perivascular routes to enable solute clearance upon exchange with brain interstitial fluid is now currently known as the glymphatic clearance pathway (Iliff and Nedergaard, 2013;Iliff et al., 2013), and is the current leading hypothesis for how the sensitive neural tissue of the CNS functions in the absence of conventional lymphatic circulation.

Despite the importance of these findings, there have been no studies that have sought to examine whether a similar pathway is found within the spinal cord. Many previous experiments examining AQP4 expression within the spine have primarily focused on

assessing injury models, such as those used to induce spinal cord compression injury (Saadoun et al., 2008) or post-traumatic syringomyelia (Hemley et al., 2013). As such, there are very few studies that have directly focused on assessing the normal localisation and distribution of AQP4 throughout the spinal cord. In a recent immunohistochemical study by Oklinski et al. (2014), AQP4 labelling in the spinal cord demonstrated the same selective localization to astrocytes that is normally observed in the brain (Nielsen et al., 1997);however, in comparison to the brain where AQP4 is highly polarized to perivascular end-feet of astrocytes, this expression was less polarized and more evenly distributed in the cell membranes around the spinal cord (Oklinski et al., 2014). Further analysing these differing patterns of expression may offer new insights into the pathogenesis of diseases such as syringomyelia and oedema, and the mechanisms that help govern fluid flow throughout the CNS.

Whilst Oklinski and colleagues (2014) study offered new insights into AQP4 expression throughout the spinal cord, these authors did not attempt to determine the identity of the blood vessels that were surrounded by AQP4; specifically whether they were arterioles, capillaries or venules. Assessing the distribution of AQP4 throughout the spinal cord in relation to markers of arterioles and venules would enable future research on the involvement of AQP4 in fluid flow within the spinal cord; specifically whether similar inflow and outflow patterns occur around peri-arterial and peri-venular spaces as seen in the brain (Iliff et al., 2012). Therefore, the aim of the current study was to perform a widespread assessment of AQP4 expression in the rat spinal cord with a specific emphasis placed upon identifying capillaries, arterioles and venules, and quantifying the surrounding AQP4 expression levels. This would enable future experiments to examine the effects that AQP4 antagonists have on fluid flow around these vessels, and allow comparisons between fluid flow within the spinal cord and brain. To address this issue, multiple labelling immunohistochemistry was performed to distinguish arterioles from venules, and capillaries were identified based upon their diameter. The surrounding levels of AQP4 expression were then quantified and compared.

Methods

2.1 Animals

Following ethical approval from the Animal Care and Ethics Committee of Macquarie University, 10 male Sprague-Dawley rats weighing 300-400g were used for immunofluorescent analysis of AQP4 expression within the spinal cord. To examine the effect of age-related changes in AQP4 expression, 5 animals were assessed at 6 weeks of age, with the remaining 5 assessed at 12 weeks of age. Animals were housed and provided access to food and water ad libitum at the Central Animal Facility located at Macquarie University for the duration of this experiment.

2.2 Tissue collection and processing

Rats were perfused with 300 mL heparinised phosphate buffered saline and 300 mL 4% paraformaldehyde in 0.1 M phosphate buffer (pH 7.4). The spinal cord was dissected out and post-fixed overnight in 4% paraformaldehyde in 0.1 M phosphate buffer, followed by cryo-protection in 30% sucrose for 48 hours. Axial slices of each spinal cord segment were obtained from four animals in both 6 and 12 week old experimental groups. Spinal segments C3, C5, C7, T2, T4, T6 and T8 collected from these rats underwent flash freezing in liquid nitrogen, whilst the remaining segments were embedded in paraffin. In addition, a spinal cord from each of the 6 and 12 week old rats was sliced longitudinally to assess vessel staining throughout various planes of the spinal cord. Frozen samples were stored in a -80°C freezer, whilst paraffin embedded samples were stored at room temperature.

2.3 Frozen tissues

For histological analysis of the frozen sections, transverse tissue slices 5 μm thick were cut using a cryostat and mounted on Superfrost Plus slides (Thermo Fisher Scientific Inc.). After cutting, slides were stored at 4°C and then dried for ~20 minutes prior to the commencement of immunohistochemical protocols. Slides were then washed in Tris phosphate buffered saline (TPBS) for 15 minutes and incubated in 50% ethanol at room temperature for 20 minutes. To block non-specific staining, 10% normal donkey serum (NDS) in TPBS was applied to all slides for 30 minutes. The sections were then incubated with polyclonal rabbit anti-rat AQP4 antibody (1:100 dilution, Novus Biologicals, Littleton, Colorado) and monoclonal mouse anti-rat endothelial cell antigen (RECA-1) antibody (1:25 dilution, Abcam, Cambridge, UK) overnight at 4°C, followed by secondary polyclonal donkey anti-rabbit IgG Alexa Fluor 488 (Life Technologies, Carlsbad, California) and polyclonal donkey anti-mouse IgG H&L DyLight® 650 (Abcam, Cambridge, UK) diluted in 1% NDS/TPBS at 1:500 and 1:400 respectively for 1 hour. All slides were then incubated with monoclonal anti α-smooth muscle actin antibody directly conjugated to the Cy3 fluorophore (Sigma-Aldrich) diluted in TPBS (1:400) at 37°C for 30 minutes. Following counterstaining with DAPI for 1 minute slides were then cover-slipped using Dako S3023 mounting medium and left to dry for 24 hours

2.4 Paraffin embedded tissues

For histological analysis of the paraffin embedded sections, transverse tissue slices 5 and 10 μm thick were cut using a microtome and mounted on Superfrost Plus slides (Thermo Fisher Scientific Inc.) and left to dry overnight at 37°C. Spinal cord sections were

deparaffinised, rehydrated and antigen retrieval was performed using 0.01 M citrate buffer (pH 6.0) at 95°C for 20 minutes. In some samples, this citrate buffer was replaced with 0.01 M Tris-EDTA buffer (pH 8.0). Sections were blocked in 10% NDS in Tris-buffered saline with the detergent Tween 20 (TBST) for 1 hour. These sections were then incubated with polyclonal rabbit anti-rat AQP4 antibody (1:50 dilution, Novus Biologicals, Littleton, Colorado) and monoclonal mouse anti-rat RECA-1 antibody (1:100 dilution, Abcam, Cambridge, UK) overnight at 4°C. In an attempt to achieve successful tissue staining, multiple secondary antibodies were tested in numerous experiments. These included polyclonal donkey anti-mouse Alexa Fluor 649, polyclonal donkey anti-mouse Alexa Fluor 549, polyclonal donkey anti-mouse Alexa Fluor 488, polyclonal donkey anti-rabbit Alexa Fluor 488, and polyclonal donkey anti-rabbit Alexa Fluor 549 (Life Technologies, Carlsbad, California), diluted 1:500 in 1% NDS/TBST for 1 hour. Unbound secondary antibodies were then removed by TBST washes, and sections were then incubated with monoclonal anti α-smooth muscle actin antibody directly conjugated to the Cy3 fluorophore (Sigma-Aldrich) diluted in TBST (1:400) at 37°C for 30 minutes. Following counterstaining with DAPI for 1 minute slides were then cover-slipped using Dako S3023 mounting medium and left to dry for 24 hours

2.5 Imaging and analysis

Slides were visualised using a fluorescence microscope (Zeiss Z2, Gottingen, Germany) and images were captured and processed at 100× and 630× magnification using Zen 2012 Axiovision software. ImageJ 1.48 (NIH,USA) was used to measure the mean pixel intensity for AQP4 expression around arterioles, venules and capillaries in grey and white matter. In order for images to be acceptable for analysis, it was mandatory that RECA-1 staining was present around the entire circumference of the targeted vessel. Expression was manually calculated by drawing around each vessel using freehand selection tools available in ImageJ software. To reduce any possible biases the investigator was blinded to the age of the animal, and whether the vessel was observed in grey or white matter. In addition, a distance of 3 microns was measured around the outside of each vessel wall, and only staining that was located within this region was used in the analysis. This ensured that all AQP4 expression readings were obtained under the same parameters and reduced the potential influence of other stained cell membranes inflating or deflating the mean pixel values as much as possible.

Arterioles were classified as vessels whose diameter was less than 50 μm and indicated staining of both RECA-1 and α -smooth muscle actin antibodies. Venules were classified as vessels whose diameter did not exceed 50 μm, and presented RECA-1 staining with the absence of α-smooth muscle actin antibodies. Capillaries were defined as vessels with a diameter less than 6.5 μm with the presence of RECA-1 staining. A total of 807 vessels were identified during this study; 517 were located in grey matter and 290 in white matter. Of these images a total of 302 met the requirements to be acceptable for analysis. This resulted in 215 vessels examined in grey matter compared to 87 in white matter. A total of 149 images were analysed for 6 week old animals and 153 images for 12 week old animals (Figure 1.).

2.6 Statistics

AQP4 expression in 6 and 12 week old animals was compared using two-way analysis of variance (ANOVA), whereby mean pixel intensity was examined across both age

and brain region between groups. In addition, AQP4 mean pixel intensity for all arterioles, venules and capillaries were compared using a univariate ANOVA to determine the overall difference in expression between these vessels. An unpaired t-test was performed to compare the differences in AQP4 expression between all grey and white matter vessels. Lastly, linear regressions were performed to examine the relationship between vessel diameter and AQP4 expression. Post-hoc Bonferroni corrections were performed to adjust for multiple comparisons in all statistical tests except the t-test. A probability value <0.05 was considered statistically significant. Software used for data analysis included Excel (Microsoft, Redmond, WA) and GraphPad Prism 5 (GraphPad Software, La Jolla, California).

Results

3.1 Staining

Successful staining of all antibodies was achieved in all frozen tissue sections. Paraffin tissue sections successfully stained for AQP4, SMA-Cy3 and DAPI, however, as numerous RECA-1 protocols failed these sections were not included for analysis as they did not allow vessels to be categorized and identified appropriately.

3.2 Overall AQP4 staining intensity in grey and white matter

Mean pixel intensities obtained for all vessels in grey and white matter, irrespective of vessel type and age are shown in Figure 2. An unpaired t-test revealed a significant difference in expression of AQP4 between these areas of the spinal cord, with vessels in grey matter demonstrating higher AQP4 expression (M = 15294.68, SD = 8590.711) in comparison to those in white matter (M =12956.50, SD = 7788.32) $p = 0.029$.

3.3 Effect of age on AQP4 staining intensity around arterioles

Mean pixel intensities obtained around grey and white matter arterioles for 6 and 12 week old animals are shown in Figure 3. An example of grey and white matter images analysed for both age groups are presented in Figures 4. and 5. respectively. A two-way ANOVA revealed no significant differences in AQP4 expression between grey and white matter ($p = 0.068$), whilst a significant overall difference between the two age groups was observed $F(1, 121) = 5.75$, $p = 0.018$. No interaction was observed between these variables ($p = 0.66$). Post-hoc analysis revealed that 6 week old animals display significantly higher mean pixel intensities around grey matter arterioles compared to 12 week old animals ($p < 0.05$).

3.4 Effect of age on AQP4 staining intensity around venules

Mean pixel intensities obtained around grey and white matter venules for 6 and 12 week old animals are shown in Figure 6. An example of grey and white matter images analysed for both age groups are presented in Figures 7. and 8. respectively. A two-way ANOVA revealed no significant differences between AQP4 expression in grey and white matter ($p = 0.12$), however, a significant overall difference in AQP4 expression was observed between the two age groups $F(1, 51) = 28.76$, $p = <0.0001$. No interaction was observed between these variables ($p = 0.31$). Post-hoc analysis revealed that 6 week old animals displayed significantly higher mean pixel intensities around both grey matter ($p < 0.005$) and white matter venules compared to 12 week old animals ($p < 0.005$).

3.5 Effect of age on AQP4 staining intensity around capillaries

Mean pixel intensities obtained around grey and white matter capillaries for 6 and 12 week old animals are shown in Figure 9. An example of grey and white matter images analysed for both age groups are presented in Figures 10. and 11. respectively. A two-way ANOVA revealed no significant differences between AQP4 expression in grey and white matter ($p = 0.71$), whilst a significant overall difference in AQP4 expression was observed between the two age groups $F(1, 118) = 27.35$, $p = <0.0001$. No interaction was observed between these variables ($p = 0.15$). Post-hoc analysis revealed that 6 week old animals displayed significantly higher mean pixel intensities around both grey matter ($p < 0.005$) and white matter capillaries compared to 12 week old animals ($p < 0.0001$).

3.6 Overall AQP4 staining intensity around arterioles, venules and capillaries

Mean pixel intensities obtained around all arterioles, venules and capillaries analysed in this study, irrespective of age and location within the spinal cord are shown in Figure 12. A one-way ANOVA revealed that no significant differences existed between the mean pixel intensities of these vessels $F(2, 299) = 1.36$, $p = 0.26$.

3.7 Effect of arteriole diameter and AQP4 expression

Correlations between the diameter of all arterioles and their mean pixel values are presented in Figure 13. A significant negative correlation was observed between the size of the arteriole ($M = 16.95$, $SD = 9.27$) and the average amount of surrounding AQP4 expressed ($M = 15355.30$, $SD = 9102.49$), $r(123) = -0.20$, $p = 0.029$; indicating that as the diameter of arterioles increases, the average amount of AQP4 surrounding decreases.

3.8 Effect of venule diameter and AQP4 expression

Correlations between the diameter of all venules and their mean pixel values are presented in Figure 14. No significant correlations were observed between the size of the venule ($M = 11.76$, $SD = 4.46$) and the average amount of surrounding AQP4 expressed ($M = 13119.10$, $SD = 7533.7$), $r(53) = 0.068$, $p = 0.62$.

3.9 Effect of capillary diameter and AQP4 expression

Correlations between the diameter of all capillaries and their mean pixel values are presented in Figure 15. No significant correlations were observed between the size of the capillary ($M = 5.029$, $SD = 1.01$) and the average amount of surrounding AQP4 expressed ($M = 14545.60$, $SD = 8037.89$), $r(120) = -0.16$, $p = 0.08$.

Discussion

The overall pattern of AQP4 expression in the spinal cords examined in this study was similar to those reported previously (Nesic et al., 2006;Oklinski et al., 2014). In grey matter, AQP4 immunolabeling was the strongest around the central canal, the outer lamina of the dorsal and ventral horns, and in the glia limitans; whereas in white matter, AQP4 was expressed in a radial pattern protruding from the grey matter to the glia limitans (Fig. 16). This AQP4 expression pattern was similar throughout all cervical and thoracic sections of the spinal cord that were examined. As AQP4 is highly polarized to the membranes of astrocytes (Noell et al., 2009), previous studies examining AQP4 expression in rat (Nesic et al., 2006), mouse (Oshio et al., 2004) and human tissue samples (Satoh et al., 2007), have all used glial fibrillary acidic protein (GFAP) antibodies to distinguish astrocytes from other glial cells. However, in the present study, tissue sections were not stained using this antibody for a number of reasons. Firstly, a primary aim of this study was to identify specific microvasculature within the spinal cord. As such, an emphasis was placed upon localising vessels in grey and white matter and identifying them as either arterioles, venules or capillaries. As the astrocytic localisation of AQP4 has been documented extensively in previous studies (Potokar et al., 2013;Oklinski et al., 2014), it was not a direct priority to establish a working protocol that included the GFAP antibody in the current experiment. That being said, as an effective methodology for distinguishing vessels was successfully developed in this investigation, the inclusion of the GFAP antibody in additional experiments may provide further insights into the expression of AQP4 around spinal cord microvasculature. Unfortunately, due to the degree of difficulty in achieving successful staining in both frozen and paraffin tissue sections, the time to stain using other antibodies was limited. Furthermore, the technical aspects of performing a quadruple labelled staining would require additional time to evaluate the optimal protocol for use. Upon establishing a successful staining procedure for frozen tissue sections, and completing the subsequent analysis of all cervical and thoracic segments, the amount of antibodies remaining in order to perform additional experiments on samples using GFAP, RECA-1 and AQP4 was not adequate due to the high concentrations required in the protocol. Despite these shortcomings, previous studies examining AQP4 expression within the spinal cord have shown that AQP4 is expressed in spinal cord astrocytes that surround blood vessels and neurons (Rash et al., 1998;Oshio et al., 2004;Vitellaro-Zuccarello et al., 2005). As such, in the current study we can assume that the AQP4 expression observed around the vessels that we imaged, reflects the commonly reported astrocytic staining pattern.

In the current study, higher levels of AQP4 expression were detected around grey matter vessels compared to white matter vessels when mean pixel values were assessed irrespective of age differences and the type of vessel observed (Fig. 2). Previous AQP4 immunolabeling experiments have documented differences of AQP4 expression in grey and white matter with similar results. Protein and tissue microarrays conducted on human tissue samples have revealed that throughout the CNS and spinal cord, AQP4 expression is lower in the white matter compared to the grey matter (Mobasheri et al., 2007). A similar pattern has also been documented in human immunohistopathological studies, whereby higher AQP4 staining was observed in spinal cord grey matter tissue in contrast to white matter (Misu et al., 2007). The presence of astrocytic end-feet surrounding capillaries has previously been reported as a key factor influencing dense AQP4 staining (Oshio et al., 2004). As capillaries are more numerous in the grey matter compared to white matter in the spinal cord, this may explain some of the variation that exists in expression between these regions (Turnbull, 1971). It is believed that these astrocytic end-feet allow changes in the vascular endothelium,

enabling fluid flow from the blood-brain barrier and blood-spinal cord barrier to occur; an important process involved in the regulation of water homeostasis for both brain and spinal parenchyma (Nicchia et al., 2004;Hemley et al., 2012). Further support for increased AQP4 expression in grey matter has been inferred from spinal cord injury studies. Self-destructive swelling and oedema are common physiological responses following spinal cord injury (Ducker and Hamit, 1969). The results of acute injury MRI studies have demonstrated that spinal eodema is most prominent in the grey matter of the cord, coinciding with the increased AQP4 expression found there as opposed to the white matter (Shepard and Bracken, 1999).

However, in the current study, when additional factors were included in the statistical analysis; such as whether the vessel being surrounded by AQP4 was an arteriole, venule or capillary, no significant differences were found between grey and white matter AQP4 expression (Figs. 3, 6, 9). These results are surprising, as previous studies throughout the literature commonly compare the total level of protein expression in the brain and spinal cord without investigating expression around microvasculature structures. To further explore the relationship between vessel type and AQP4 staining intensity, the average levels of AQP4 immunoreactivity were calculated for all arterioles, venules and capillaries to determine whether a specific vessel type was associated with the highest levels of protein expression. Interestingly, no significant differences were observed in AQP4 expression between each of these vessels; suggesting an even distribution of AQP4 around vessels throughout the spinal cord (Fig. 12). These results differ from the only other existing study conducted by Iliff et al. (2012), which examined perivascular AQP4 expression at astrocytic end-feet around arterioles, venules and capillaries in the rodent brain. These authors found that peri-arterial end-feet expressed significantly less AQP4 than peri-capillary or peri-venular end-feet. Previous immunolocalisation studies have noted that AQP4 labelling in the spinal cord demonstrates an even distribution around astrocytic cell membranes in contrast to the brain, where it is highly polarized to astrocytic end-feet (Oklinski et al., 2014). Therefore, although our results differ to those reported by Iliff et al. (2012), they appear to reflect the potential differences that may exist in AQP4 cellular localisation between the brain and spinal cord. Whether this can entirely be explained by variation in AQP4 polarization around astrocytes remains to be seen.

There are, however, a number of variables related to the methodology used in the current investigation that may also account for the differences observed in AQP4 expression around arterioles, venules and capillaries. Firstly, to help distinguish the identity of all the vessels analysed in this study, an inclusion criterion was incorporated into the experimental design which required the diameter of each vessel to be recorded during inspection. Arterioles are generally considered to have diameters ranging up to approximately 100 μm (Rhodin, 1967), after which, they are largely considered to be arteries (Strandness et al., 1964;Jones et al., 1995). In order to distinguish arterioles from venules and capillaries in this study, it was imperative to be able to detect the presence or absence of α-smooth muscle actin, a differentiation marker of smooth muscle cells (Skalli et al., 1989), around each vessel. It has previously been reported that arterioles with diameters as small as 7 μm show a single layer of smooth muscle cells in the human brain (Shiraishi et al., 1990), and that it is not until the diameter of these vessels exceeds 50 μm that several layers of smooth muscle become present (Rhodin, 1967). As such, a diameter of 50 μm was selected as the maximum value for inclusion as it would ensure consistency between the numbers of smooth muscle cell layers present in all arterioles examined. In this study, capillaries were defined as vessels with diameters smaller than 6.5 μm; a size that has commonly been reported as representative for these vessels throughout the brain and spinal cord (Quaia and Bartolotta, 2005;Jeong et al., 2006). To maintain consistency with arterioles classification, the maximum diameter

acceptable for venules was also limited to 50 μm. Upon further examination, the exclusion of vessels that exceeded this diameter from our study may have accounted for the observed differences in AQP4 expression around arterioles in comparison to Iliff et al. (2012). When the relationship between the diameters of each vessel and their corresponding AQP4 immunolabeling intensity was assessed, a significant negative correlation was found between arteriole diameter and AQP4 expression (Fig. 13). Therefore, as the diameter of arterioles increased, a subsequent decrease was also observed in the average expression of AQP4 around the vessel. Furthermore, no significant correlations were observed between venule diameter (Fig. 14) or capillary diameter (Fig. 15) and AQP4 expression. These trends all reflect those reported by Iliff and colleagues (2012), and therefore, it appears that the arterioles examined in their study may have been of a larger size and thus demonstrated reduced expression of AQP4 around each vessel. In the current experiment the average diameter of arterioles was approximately 17 μm (Figure 17). Unfortunately, we were not able to appropriately analyse many of the larger vessels that did not exceed 50 μm in this study, as RECA-1 antibody staining would be present around specific areas of these vessels, but in most cases would not completely label the entire circumference of the vessel. As we required the entire vessel wall to be visible, these vessels were subsequently excluded from analysis. The exclusion of these vessels was a necessary process in order to ensure consistency between the measurements acquired throughout the course of this investigation; specifically so that the diameter of each vessel could be correctly identified without confusion of where the vessel walls started and finished. This was of particular importance for determining vessel identity in the white matter, as a large number of the vessels observed in this area demonstrated the penetrating pattern shown in Fig. 18. As the diameter of these vessels could not be established due to this alignment, arterioles, venules and capillaries could not be determined without uncertainty. As Iliff et al. (2012) did not mention the sizes of the vessels they examined in their study, we are unable to explore this possible source of variation any further.

The use of transgenic animals may perhaps be another source of variation that accounts for some of the discrepancies between results in our respective investigations. In their study, Iliff and colleagues (2012), utilised a two-photon laser scanning microscope to assist with their identification of arterioles, venules and capillaries. Whilst this form of microscopy provides slightly lower spatial resolution compared to other methods such as confocal microscopy, it enables three-dimensional imaging of specimens in vivo, provides deeper tissue penetration and results in less photodamage occurring to the sample (So, 2001). In order to visualise astrocytic end-feet in vivo, these authors used FVB/N-Tg mice, which overexpress fluorescent proteins under the control of astrocyte specific GFAP promoters (Huang et al., 2008). In addition to this, Iliff and colleagues (2012) were able to distinguish arteries, arterioles, veins and venules from each other in the brain without the need of additional histochemical labelling by using transgenic Tie2-GFP:NG2-DsRed mice. These mice label all blood vessels with GFAP and DsRed, which subsequently allows arterioles, venules and capillaries to be identified based upon DsRed patterns of expression. Arterioles and arteries exhibit a dense circumferential pattern whilst capillaries, veins and venules all express low levels of DsRed staining. By having access to these animals and advanced imaging devices, analysis of vessels did not appear to suffer from possible limitations associated with vessel size, position or identity ambiguity. In comparison to mice, rat one-cell embryos have less visible pronuclei which makes transgene injection more difficult. In addition to this, the survival rate of these injected rat embryos are low; resulting in greater financial demands and time to develop these transgenic animals in comparison to mice (Charreau et al., 1996). As we were unable to use any transgenic animals in this study to help

identify arterioles, venules and capillaries, we instead relied upon the presence of RECA-1 antibodies to identify microvasculature, and distinguished between vessel types based upon their diameters and the presence or absence of α-smooth muscle actin. Pericytes, also known as Rouget or peri-endothelial cells, wrap around the endothelial cells of capillaries and venules throughout the body (Dore-Duffy, 2008). These cells are key to ensuring homeostasis in the CNS, regulation of capillary blood flow, and maintenance the blood-brain barrier (Winkler et al., 2011). Originally recognized by their distinctive shape and location, today, pericytes are commonly identified by molecular markers such as α-smooth muscle actin and desmin (Morikawa et al., 2002). As pericytes are multicomponent cells that retain the capacity to differentiate into other types of cells; such as smooth muscle cells (Nehls and Drenckhahn, 1993), the presence of α-smooth muscle actin is believed to be of particular importance for vessel contraction in vascular function (Lee et al., 2007). Although a smooth muscle layer is traditionally believed to be absent from capillaries and post-capillary venules (Lee et al., 2007), previous studies such as Morikawa et al. (2002) have documented the presence of α-smooth muscle actin around both arterioles and venules in the rat pancreas; however it is important to note that these researchers did not explain their rationale for distinguishing between these two vessel types in their investigation. The occurrence of smooth muscle cells in the walls of venules located in the rat brain has also been noted in experiments performed by Saubamea et al. (2012), however, the resulting staining these researchers observed around venules was considered too faint to impact the classification of vessels in their study. Therefore, due to the presence of α-smooth muscle actin within pericytes that surround the capillaries and veins, there is potential that this expression may result in some capillaries and venules being misclassified as arterioles. To ensure this variable did not influence the classification of vessels in our experiment, we analysed each sample using the same brightness and contrast parameters; this helped to establish a common threshold that allowed the staining of α-smooth muscle actin to be consistent between all animals. As such, it appears unlikely that misclassifications of vessel types have occurred within our study.

Differences observed in AQP4 expression concerning the brain and spinal cord raise interesting questions regarding how fluid flows through these sites. Previous experiments have demonstrated that subarachnoid CSF enters the brain along paravascular spaces surrounding penetrating arteries (Rennels et al., 1985;Iliff et al., 2013). The increased expression levels of AQP4 observed around venules by Iliff et al. (2012) have been suggested to help maintain a low resistance clearance pathway that facilitates outflow around peri-venular spaces in the brain, into subarachnoid spaces. In contrast, little is currently known regarding fluid movement within the spinal cord. Results from tracer studies by Stoodley et al. (1996) have previously demonstrated that a normal flow of fluid occurs from the spinal subarachnoid space, through perivascular spaces into the central canal. It is been postulated by Milhorat (1992) that this pathway through the central canal functions as a drain for toxic or metabolic waste products. As such, dysfunction of the central canal has frequently been associated with the pathogenesis of CSF disorders such as syringomyelia (Muthukumar, 2012), although the extent to which this fluid filled space influences the development of this condition has proven to be a controversial point of discussion. Autopsy studies have indicated that the central canal gets progressively obliterated with age (Yasui et al., 1999), and large degrees of stenosis are particularly predominant in individuals past the age of 60 (Milhorat et al., 1994). Therefore, it has been suggested that central canal occlusion is not involved in the development of syringomyelia in adults, however, the appearance of this obstruction in younger individuals is believed to have an influence on the pathogenesis of this disease (Hashizume et al., 2001). Thus it appears that during maturity other outflow pathways

compensate for a potential reduction in fluid movement around the central canal. In the current study, a large amount of AQP4 expression was observed around the central canal at all spinal levels examined. As such, this staining may represents a pathway that assists in CSF outflow from the spinal cord, similar to how Iliff and colleagues (2012) speculated that high levels of AQP4 expressed around venules facilitates outflow around those vessels. Longitudinal studies assessing the effect of age on patency and expression of AQP4 in this region of the spinal cord could further confirm this hypothesis using labelled tracers.

In addition to comparing levels of AQP4 expression in grey and white matter, and assessing the staining intensity surrounding arterioles, venules and capillaries, this study also examined the effect of age-related changes in AQP4 expression using 6 and 12 week old animals. To determine whether developmental variances were present, differences in AQP4 staining around grey and white matter arterioles, venules and capillaries were compared between age groups. For both 6 and 12 week old animals, the levels of expression observed in the grey matter were comparable to those recorded in the white matter; for example, in 6 week old animals AQP4 expression in grey matter arterioles was not significantly different to the expression seen in the corresponding white matter arterioles. However, noteworthy variances in AQP4 expression arose when mean pixel values were compared between age groups. We found that 6 week old rats expressed significantly higher amounts of AQP4 around grey matter arterioles, venules and capillaries, and white matter venules and capillaries, in comparison to 12 week old rats (Figs. 3, 6, 9). At the present, there are no previous experiments that have documented the development of AQP4 expression in the spinal cord from birth to maturity. As such, most of our understanding comes from studies examining the expression of AQP4 within the brain. The blood-brain barrier is a multicellular vascular structure that helps to maintain a constant, optimal environment for neuronal function (Betsholtz, 2014). This is achieved by separating the CNS from peripheral blood circulation, and controlling the influx and efflux of molecules and ions that pass into and out of the CNS (Obermeier et al., 2013). The role of AQP4 during the development of the blood-brain barrier has previously been investigated in the optic tectum of chick embryos and newly hatched chicks by Nico et al. (2001). By means of western-blot, reverse transcriptase-polymerase chain reaction, immunohistochemistry and high-resolution immunogold electron microscopy, these authors demonstrated that AQP4 expression around astroglial cells occurs in parallel with the maturation and functioning of the blood-brain barrier. However, in another study conducted by Wen et al. (1999), who examined post-natal expression of AQP4 throughout the rat cerebellum using a similar assortment of methods, it was found that AQP4 was expressed in very low levels during the first week of post-natal development, and it was not until the second week that a prominent increase in expression was actually observed. These discrepancies regarding the pre- and post-natal expression of AQP4 can be explained by differences in the time of development of the brain-blood barrier in these two animals. In birds, the development of this barrier is known to be completed in embryonic life (Roncali et al., 1986), whereas in rats this development is finalised in post-natal life, when the extracellular space is not large enough to accommodate ion and water flux (Schulze and Firth, 1992;Wen et al., 1999). Together, these studies suggest that AQP4 expression around astrocytes begins to occur simultaneously with the development of the blood-brain barrier.

The blood-spinal cord barrier is believed to be the functional equivalent of the blood-brain barrier as it helps to provide a specialised microenvironment for the cellular constituents of the spinal cord (Bartanusz et al., 2011). However, empirical evidence has indicated that numerous morphological and functional differences exist between these two types of barrier structures. Using radioactive labelling techniques, Pan et al. (1997) have demonstrated that cervical, lumbosacral and thoracic regions of the spinal cord, all exhibit

greater permeability to cytokines in comparison to the brain. Furthermore, following culture and immunocytochemical analysis of the spinal cord microvascular endothelial cells -- which form the blood-spinal cord barrier, Ge and Pachter (2006) have observed the reduced expression of several proteins that are also found in the brain-blood barrier; including the efflux transporter P-glycoprotein and the tight-junction associated protein occludin. These results suggest that the increased permeability of the blood-spinal cord barrier, in comparison to the brain-blood barrier, may have arisen due to differences in cell junction protein expression around endothelial cells (Bartanusz et al., 2011). At the present, the existing knowledge regarding the volume of CSF located within the spinal cord is extremely limited. In the normal healthy adult, the total volume of CSF present throughout the CNS is believed to be approximately 150 mL (Rizvi and Coyle, 2011). Previous experiments performed using MRI have revealed that a large degree of variability exists in total human spinal CSF volume (Sullivan et al., 2006), with figures ranging from between 81 to 120 mL (Hogan et al., 1996;Edsbagge et al., 2011). As such, it appears that a larger volume of CSF is present around the spinal cord at any time point in comparison to the volume located in and around the brain. Subsequently, it can be speculated that the distribution of AQP4 within the spinal cord may differ to that of the brain due to an association with the movement of a greater volume of fluid, a process that may potentially be supported by more permeable barrier layers (Pan et al., 1997). Therefore, these findings may explain why a more uniform distribution of AQP4 expression was observed around the vessels within the spinal cord in the current study, and why these results do not conform to those documented in the brain. Due to these differences in protein expression, and the lack of experiments that have documented the development and growth of AQP4 in the spinal cord, it is important to conduct investigations in the future to determine whether significant differences arise in the development of AQP4 within the brain and spinal cord.

In regards to the age related differences of AQP4 expression that were observed in the current investigation, there is only one existing study that has previously documented changes using a similar age bracket. In a recent experiment by Gupta and Kanungo (2013), reverse transcription polymerase chain reaction and immunoblotting were performed on the cerebral and cerebellar cortices of post-natal and adult mice. These authors observed a lack of AQP4 expression in newborn mice, followed by significant increases in expression levels from 15 days until the completion of the post-natal period when mice were 45 days old; reflecting the findings previously published by Wen and colleagues (1999). The expression of AQP4 observed at 45 days appeared to remain consistent during the development of the mice, as similar levels were also documented in animals that were 20 weeks old. However, the highest levels of expression recorded in this study were seen in 70 week old mice; the oldest animals included in the experiment. This difference was believed to arise due to the narrowing of extracellular space volume in the brain, a naturally occurring phenomenon that is the result of cellular morphology changing as the body ages (Sykova et al., 1998). Therefore, Gupta and Kanungo (2013) concluded that the age-related increase of AQP4 expression may reflect the increased need to maintain water homeostasis due to the burden associated with regulating ion and neurotransmitters in narrower extracellular spaces.

In contrast to the results obtained by Gupta and colleagues (2013), our analysis indicated that within the spinal cord the highest levels of AQP4 expression are observed following the completion of the post-natal development period, and it appears that expression around all vessels, excluding white matter arterioles, decreases with age (Figs. 3, 6, 9). There are a number of possible explanations that may account for these observed differences. As previously mentioned, the blood-spinal cord barrier is believed to be more permeable than the blood-brain barrier (Bartanusz et al., 2011). The reported increase of AQP4 expression in

older mice that Gupta and colleagues (2013) reported, was assumed to be in response to difficulties maintaining water homeostasis. As such, it can be speculated that the increased permeability of the spinal cord may reduce the potential burdens associated with fluid maintenance during aging. Further differences in these results may also be attributed to methodology. In the relevant publications that have been cited, previous experiments have calculated the total values of AQP4 expression throughout entire brain regions. As previously noted, we were only able to compare AQP4 expression around vessels that met our inclusion criteria. Therefore, it may be possible that a greater number of vessels located around areas that demonstrated increased AQP4 staining; such as the dorsal and ventral horns, were included in the analysis of 6 week old compared to 12 week old rats. In order to successfully account for these differences, future experiments could incorporate a grid system, whereby each vessel observed could be mapped to an exact co-ordinate within the spinal cord. This would enable an accurate comparison of AQP4 expression between multiple age groups, and the developmental changes that may occur at specific regions in the spinal cord could be easily investigated.

A potential improvement that could be made to our experimental design that could help confirm whether significant differences existed in the overall levels of AQP4 expression between age groups, would be to assess expression levels in a larger range of age groups using additional analytical techniques. Western blot analysis is a rapid and sensitive technique that allows for the detection and characterisation of proteins based upon the specificity of antigen-antibody recognition (Gallagher and Chakavarti, 2008). In previous studies, immunoblot analysis has been used to confirm changes in AQP4 expression that have arisen in the brain following interference by RNA (Badaut et al., 2011), structural damage (Lu et al., 2013), and the development of brain tumours (Wang and Owler, 2011). Although Western blotting is a valuable technique to verify the presence of specific proteins in extracted cell bodies, the results obtained using this method are semi-quantitative, as a standard curve with known concentrations of the target protein, or samples relative to a control sample are required for comparisons (Heidebrecht et al., 2009;Mahmood and Yang, 2012). In comparison to Western blots, enzyme-linked immunosorbent assays (ELISA) are another sensitive and protein specific method that can be used to analyse quantitative results (Corrales and University, 2008). ELISA assays have previously been used to examine differing concentrations of AQP4 in communicating and obstructive hydrocephalus (Castaneyra-Ruiz et al., 2013). In addition, newly developed commercial assays have demonstrated higher sensitivity for detecting AQP4 compared to standard immunohistochemical procedures (Jarius et al., 2012). Previous experiments have encountered increased success upon utilising a combination of both tissue staining and ELISA assays to assess expression changes (Beck et al., 2005). Therefore by adapting this dual method scheme into our current protocol, it may provide a more in-depth analysis of the changes that occur in protein expression around vessels in spinal cord and brain with regard to ageing. In addition to helping confirm levels of AQP4 expression between different subject groups, other techniques such as *in situ* hybridization could be used to provide additional support for the localisation of AQP4 around vessels in the spinal cord. Whilst originally developed to localise genes on chromosomes, the application of *in situ* hybridization techniques to the mammalian brain revolutionised methods of detecting intracellular RNA expression (Wisden and Morris, 2002). By using labelled complementary DNA or RNA stands, specific DNA or RNA sequences are able to be localised in tissue and quantified. This technique has previously localised AQP4 transcripts in the pial surface and ependymal cells (Venero et al., 1999); further supporting the importance of AQP4 mRNA in structures associated with fluid regulation. As immunohistochemistry detects the presence of proteins,

whilst *in situ* hybridization detects target RNA or DNA sequences, a combination of both techniques would provide a thorough assessment of the distribution of AQP4 within the spinal cord. This could potentially be achieved by replacing the AQP4 antibody used in the current protocol with AQP4 cDNA. As such, vessels would still be able to be identified based upon the presence of RECA-1 and α-smooth muscle actin antibodies, and potential differences in AQP4 expression in these cells could be examined. Therefore, by expanding our methodology in subsequent experiments, and examining expression over a larger age group such as those inspected by Gupta and Kanungo (2013) we could prove with greater certainty whether differences in AQP4 expression arise due to developmental changes, or are attributed to higher levels of expression around specific microvasculature structures.

Despite the fact that we have addressed many of the potential limitations in this study, and followed precautionary procedures to avoid possible sources of conflict over the course of this investigation, there were some shortcomings that we were unable to resolve. The largest drawback observed in this experiment was the failure to establish a working protocol to visualise microvasculature in paraffin embedded sections. Whilst we were successfully able to stain these tissue samples using AQP4 and α-smooth muscle actin antibodies, this was never achieved using RECA-1 antibodies due to non-specific, heavy background staining. Numerous tests were performed to determine the possible source of this problem. Firstly, a variety of secondary antibodies were examined at different concentrations to determine whether this was the cause of the negative staining. When none of these proved to be successful; despite being raised against the same species used in the primary, additional tests were performed to assess whether the reason for unsuccessful staining was the primary antibody itself. Various antibody dilutions and incubation times were assessed, however, none of these offered any improvement to the staining observed. When the same primary antibody was tested in frozen embedded tissue sections, a positive staining result was observed. This indicated that the problem we had been encountering may not have been specifically related to the antibody itself, but a consequence of antigen retrieval. When using paraffin embedded sections, in order for successful staining to occur, the paraffin must first be completely removed using solvents such as xylene before application of the antibodies. If the paraffin is not removed, this can prevent antibodies from reaching their target antigens, and therefore result in non-specific staining (Goswami, 2012). Therefore, in addition to several secondary antibodies being tested to see if they worked in paraffin embedded spinal cord tissues, multiple forms of antigen retrieval were also examined. Unfortunately neither of these alterations provided any improvements to the staining observed. Slice thickness is an important variable to control when mounting tissue on slides, as thin sections, such as those less than 3μm, are known to produce weak immunostaining, whilst extremely thick sections can result in uneven staining throughout the entire tissue sample (Yaziji and Barry, 2006). Consequently, as a last resort, we examined whether the difficulty to achieve successful RECA-1 staining was attributed to the thickness of our samples. When 5 and 10 μm slices displayed no difference in background staining, we ceased attempting to establish this working protocol. Therefore, despite numerous attempts, including replicating protocols that had previously shown successful RECA-1 staining in paraffin embedded tissues (Park et al., 2008), we could not achieve successful staining in these sections in our study This was associated with a number of drawbacks regarding our analysis of AQP4 within the spinal cord, as only half of the total tissue sections prepared could be analysed. Due to the fact that spinal segments alternated between embedding mediums; for example C3 was frozen whilst C4 was paraffin fixed, it was not possible to examine the continuous expression of AQP4 throughout the spinal cord. It should also be noted that due to our inclusion criteria, some segments of the spinal cord did not contain a large number of vessels. This prevented us from

performing direct comparisons of the levels of AQP4 expressed between each segment of the spinal cord; for example C3 and C5. As a result, data obtained from all segments had to be pooled and assessed based upon proximity to grey or white matter. Therefore, by including a larger amount of animals in future studies, it may be possible to perform assessments whereby the expression of AQP4 can be determined for each spinal level.

Despite staining protocols requiring additional stages such as de-waxing, rehydrating and antigen retrieval processes, the morphology of paraffin embedded tissues is generally regarded to be superior in comparison to frozen tissues (Shi et al., 2011). As the aim of this study was to investigate AQP4 expression around microvasculature in the spinal cord, it is unfortunate that we could not use samples that may have provided the best structural images. Due to better preservation of morphology, it is possible that more vessels would have been able to be included for analysis in this study if we could have established a working paraffin protocol. However, whilst this is a limitation, it should be noted that frozen tissue sections generally show better immunoreactivity compared to paraffin sections as antigenic preservation is superior (Beckstead, 1994). Therefore, whilst morphology may be slightly compromised in the samples we could analyse in this study, the evaluation of AQP4 expression may be more accurate compared to potential data acquired using paraffin embedded tissues.

In the current experiment we have successfully been able to identify various microvasculature structures within the spinal cord, and quantified the levels of AQP4 expression that surround them. Continuing with this research, the next important step is to investigate how these levels of expression influence the movement of fluid within the spinal cord. As previously reported, Iliff et al. (2012) observed significantly reduced movement of tracer into the brain parenchyma in AQP4 knockout mice compared to normal controls. However, whether this effect is also observed within the spinal cord has not yet been investigated. To do this, a series of experiments could be performed using fluorescently labelled tracers to examine the effects AQP4 agonists and antagonists have on the movement of fluid within the spinal cord. By including the staining protocol that we have established in the current study to differentiate microvasculature, it will be possible to investigate changes that occur in AQP4 expression, and to distinguish the vessels upon which the tracer may travel through. This could also be aided by including longitudinal slices of the spinal cord following tracer injections into animals. Whilst virtually all tissue slicing performed in this experiment involved axial cutting, one spinal cord from each of the 6 and 12 week old animal groups was sliced longitudinally. Although these sections were excluded from analysis as it was not possible to differentiate between grey and white matter, as specifications such as the depth travelled into the cord could not be assessed when mounting tissues on slides, it was possible to follow the protrusions of vessels throughout each section. By including longitudinal slices in tracer studies, it would enable better visualisation of the pathways which the tracer may travel throughout, and allow investigation into whether any diffusion into the surrounding parenchyma occurred following injection. This is an important factor to consider when using tracers to examine flow with the CNS. Previous studies have used large tracers such as albumin labelled with colloidal gold to determine penetration of subarachnoid CSF into the brain by perivascular spaces (Ichimura et al., 1991). However, the size of a tracer used to study flow can have a major impact on whether it is able to exit the perivascular space and move across the interstitium (Iliff et al., 2012). In experiments we have performed to investigate the movement of CSF in the spinal cord following thecal sac constriction (unpublished data), we have observed successful movement of far-red fluorescent Alexa Fluor 647 ovalbumin conjugate from the cervical to the thoracic nerves of the rat spinal cord. The size of this tracer is large enough to avoid rapid diffusion, yet small

enough to show intercellular pathways. As such, it would be useful to continue to assess the practicality of this tracer in AQP4 modulation experiments.

Although previous studies have utilised knockout mice to assess the effect of changes in aquaporin expression, we believe rats are a more ideal animal for studying the movement of fluid within the spinal cord. Rats are physiologically, genetically and morphologically more similar to humans than mice are (Do Carmo and Cuello, 2013). In addition, due to their larger size they are easier to integrate into spinal surgical research models. As such rats are commonly used to investigate spinal disorders such as syringomyelia (Yang et al., 2001;Kundi, 2013) and oedema following spinal cord injury (Sharma and Olsson, 1990). Therefore, as our vessel staining protocol was established in this species, it is now also possible to investigate changes that occur in AQP4 expression around microvasculature in response to trauma, and the development of diseases within the spinal cord. Such findings would provide us with a more detailed understanding of fundamental spinal fluid physiology, and the effects of common obstructions to fluid flow.

Although AQP4 is the most widely expressed aquaporin in the CNS, other aquaporins could also contribute to normal fluid flow, as well as potentially play important roles in fluid movement following spinal cord injury. At present, researchers are inquiring into the potential roles that other aquaporins may have within the brain and spinal cord; specifically aquaporin-1 (AQP1) and aquaporin-9 (AQP9). The AQP1 protein has been localised to the apical membrane of the choroid plexus epithelium in both rats (Speake et al., 2003) and humans (Longatti et al., 2004). As such, this protein is believed to play an important role in the formation of CSF within the brain (Owler et al., 2010). This is supported by data collected in experiments using AQP1-null mice, which show significant reductions of up to 25% in the production of CSF (Oshio et al., 2003). Subsequent experiments have also demonstrated that these mice have significantly reduced intracranial pressure, and improved survival rates in cold focal brain injury models (Oshio et al., 2005). As such, reduced intracranial pressure observed by down-regulation of AQP1 may have strong implications in treating CNS dysfunction. Experiments in the rodent spinal cord have also found that AQP-1 is weakly expressed in grey and white matter astrocytes (Nesic et al., 2008), and ependymal cells lining the central canal; however, more robust staining has been observed in sensory fibres of the dorsal horn using electron microscopy (Shields et al., 2007). The nociceptive withdrawal reflex is believed to be mediated by neural circuitry in the dorsal horn (You et al., 2003), and therefore AQP1 has been suggested to be involved with pain responses within the spinal cord (Nesic et al., 2008). As a strong staining of AQP4 was also observed around the dorsal horn in the current study, it would be of interest to examine both AQP1 and AQP4 expression in response to neuropathic pain, to determine if any correlations exist between these proteins within the spinal cord.

The AQP9 protein has been found to be expressed in astrocytes in the glia limitans, and endothelial cells of pial vessels (Badaut et al., 2004). As such, it has been suggested that this protein may have involvement in water transport through the brain-blood barrier (Zelenina, 2010). Following ischemia, or after traumatic brain injury, the expression of AQP9 has been shown to be up-regulated in rats (Badaut et al., 2001). A similar occurrence has previously been reported for AQP4 expression in astrocytes found in human brains with various inflammatory lesions (Aoki-Yoshino et al., 2005). Together, these reports suggest that water movements associated with maintaining homeostasis may be regulated by aquaporin expression and distribution in the brain (Waksman, 2006). Therefore, by identifying vessels using the protocol established in the current experiment, and staining for various aquaporins, injury models could assess both the effects of spinal cord damage on pain

responses, as well as fluid flow. This may provide insight into possible therapeutic approaches to treat cases of spinal cord injury. Hopefully one day, using a protocol similar to the one we have established in the current study, we will be able to stain microvasculature structures in human spinal cords to determine whether differences exist in aquaporin expression around arterioles, venules and capillaries. This type of study would be of particular importance, as with the exception of AQP4, other aquaporins such as AQP1 and AQP9 have not yet been determined to be present within the human spinal cord (Nesic et al., 2010). Due to significance that these proteins appear to have in maintaining homeostasis within the rodent spinal cord, in addition to the opportunities offered in developing new treatments to address diseases based upon their function, the challenge of locating and assessing these proteins would have substantial therapeutic implications and increase the current limited understanding of fluid flow within the spinal cord.

Collectively, the results of the current study suggest that the expression of AQP4 in the spinal cord varies to that observed in the brain. Whilst both the brain and spinal cord show higher levels of AQP4 expression around the grey matter in comparison to white matter, no overall differences were detected between AQP4 expression levels around arterioles, venules and capillaries. Significantly higher levels of AQP4 expression were found around microvasculature structures in rats following completion of the post-natal period, however this expression appears to decrease as rats mature into adulthood. The results of this study lay the foundation for future experiments to assess the effect of AQP4 antagonism on fluid flow within the spinal cord, and offer an additional method for examining AQP4 expression changes in the spinal cord following traumatic injury.

Acknowledgements

I would like to thank Professor Marcus Stoodley for providing me with the opportunity to undertake these experiments for the past year. It has truly been an incredible experience that has helped me grow as a person, and changed my perspectives of many elements associated with research.

I would also like to thank Dr. Tom Woodcock who provided me with regular assistance in the laboratory and trained me to use various techniques over the course of this study. He was always there whenever I needed aid, or simply someone to talk to. Without his advice, patience and never-ending support, this thesis would not have been possible.

Lastly I would like to give special thanks to my parents for supporting me and my decision to undertake this challenge, and my partner Roshana, who has always believed in me, even at times when I stopped believing in myself.

Other contributors

Perfusion and collection of tissue samples for 6 and 12 week old rats was performed by Dr. Tom Woodcock and Dr. Elmira Najafi. Dr. Tom Woodcock also assisted with the development and practice of the immunohistochemical procedures performed in this experiment.

Appendix

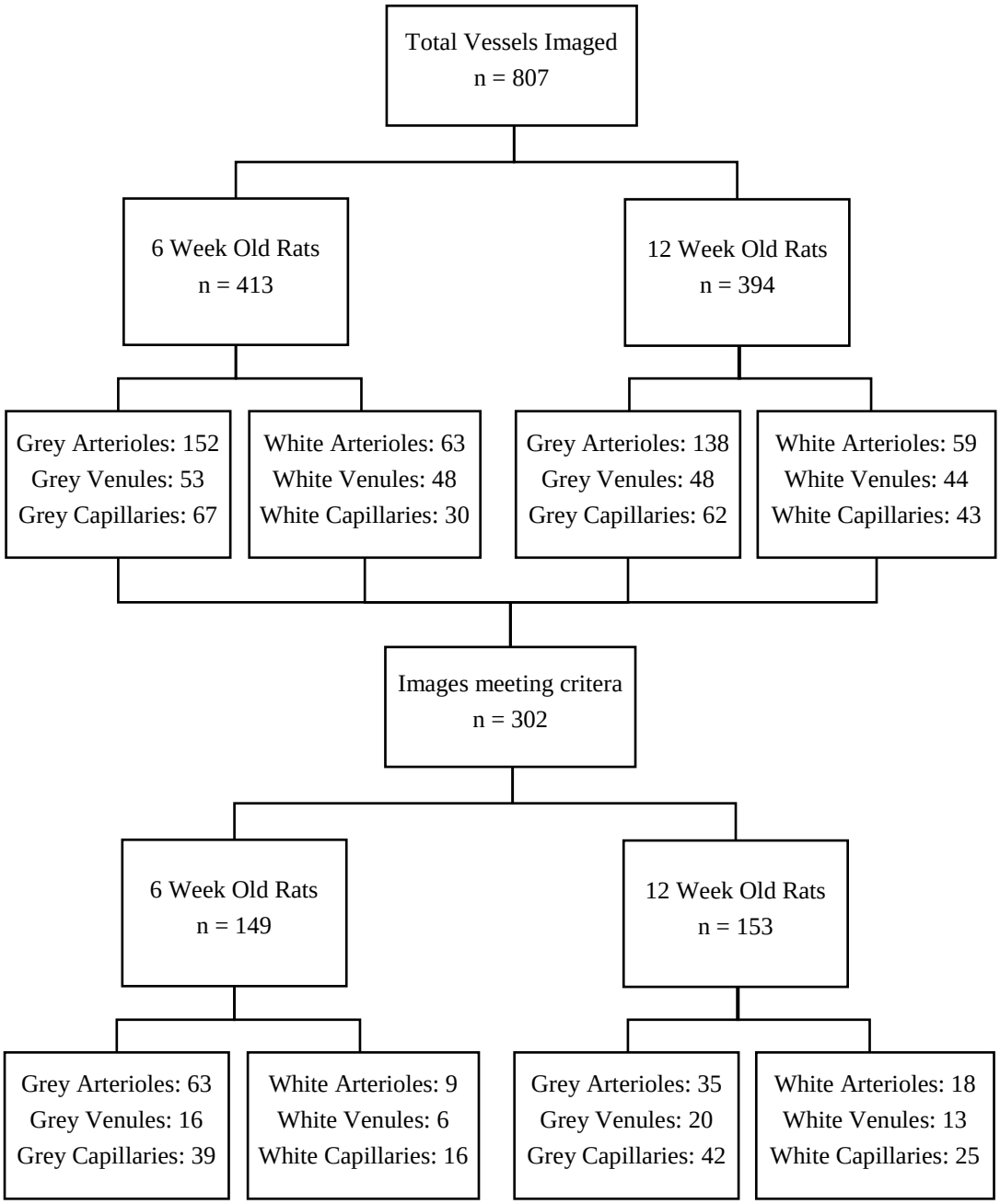

Figure 1. A flowchart depicting the total amount of images acquired in this study and the final number included for statistical analysis. RECA-1 staining was required around the entire circumference of each vessel. Arterioles were classified as vessels with diameters less than 50 μm that stained for both RECA-1 and smooth muscle actin Cy3 antibodies. Venules were classified as vessels whose diameter did not exceed 50 μm, and presented only RECA-1 staining. Capillaries were defined as vessels with a diameter less than 6.5 μm with the presence of RECA-1 staining.

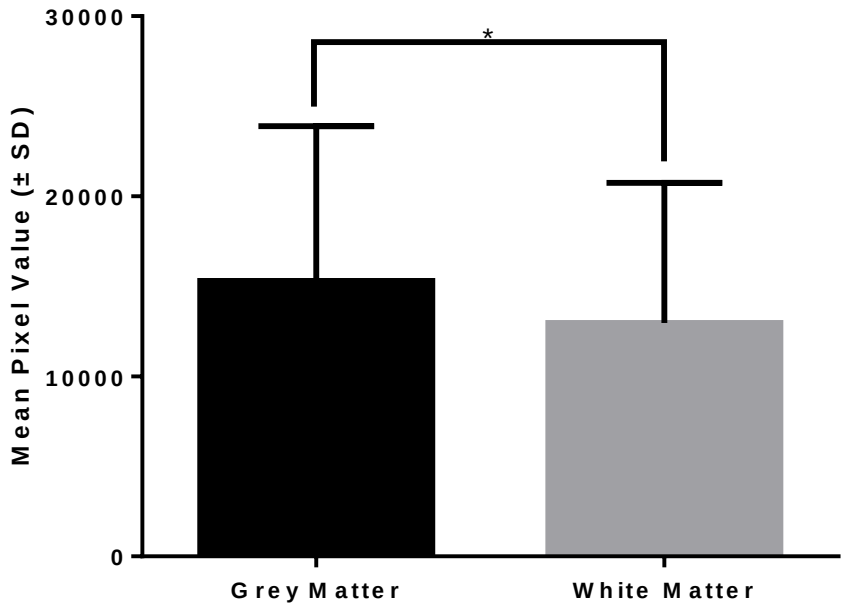

Figure 2. Calculated mean pixel values for aquaporin-4 staining around grey and white matter vessels irrespective of vessel type and age. Mean pixel intensity was determined using ImageJ software. Grey matter vessels: n = 215. White matter vessels: n = 87. * = P <0.05. Error bars indicate ± SD

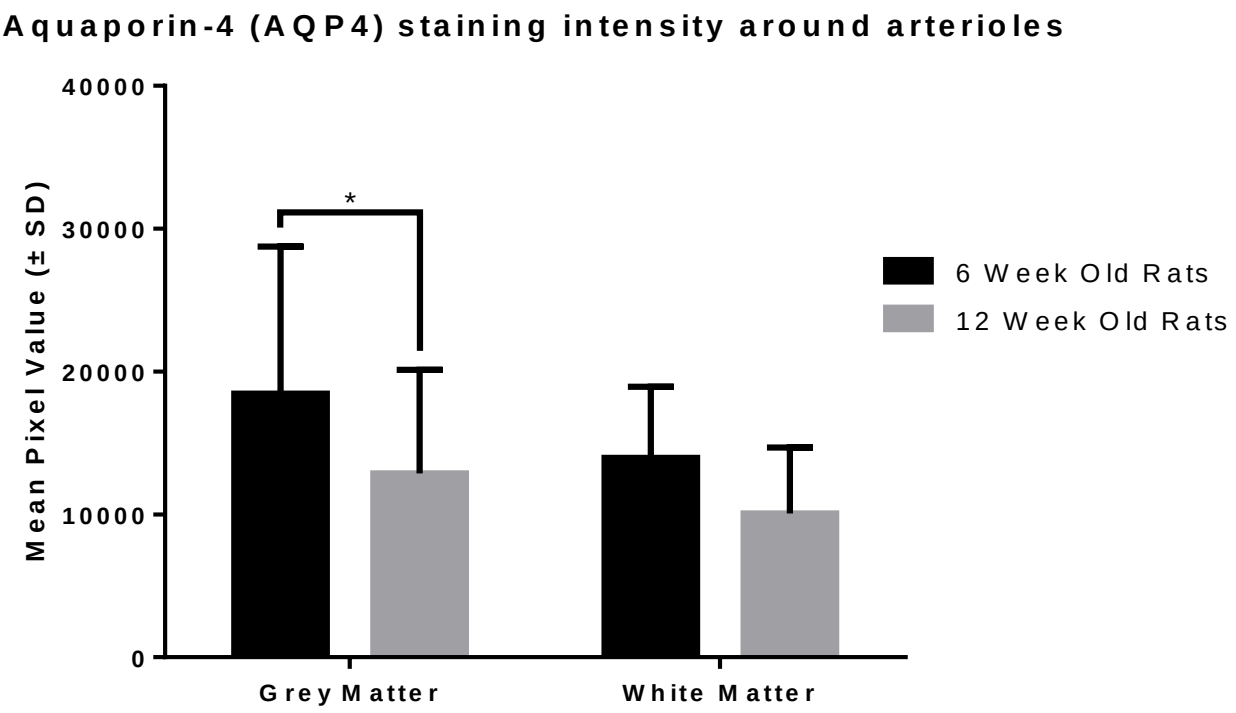

Figure 3. Calculated mean pixel values for aquaporin-4 staining around grey and white matter arterioles in 6 and 12 week old animals. Mean pixel intensity was determined using ImageJ software. Grey matter arterioles: 6 weeks n = 63, 12 weeks n=35. White matter arterioles: 6 weeks n = 9, 12 weeks n = 18. * = P <0.05. Error bars indicate ± SD

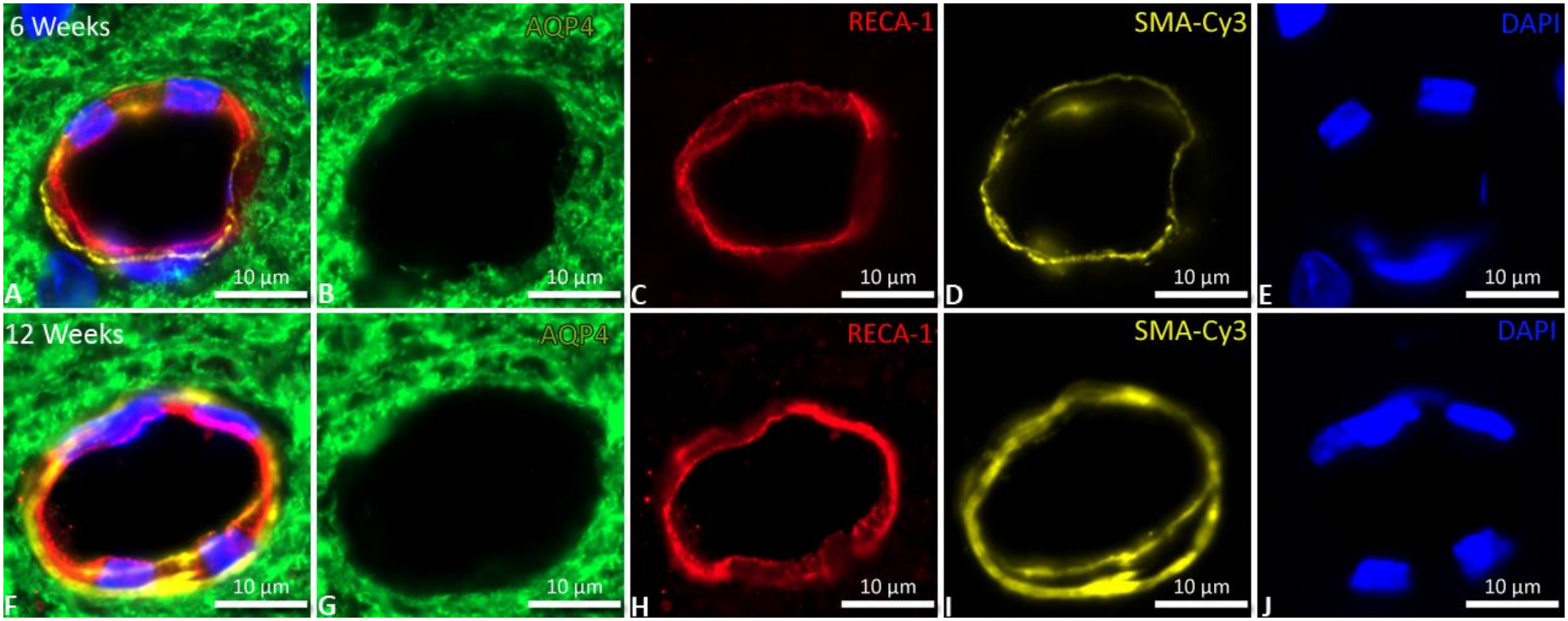

Figure 4. Examples of grey matter arterioles in 6 and 12 week old rats. (A,F) A merged stack of all antibodies assessed at 630x resolution. (B,G) Polyclonal rabbit anti-rat AQP4 antibody (1:100). (C,H) Monoclonal mouse anti-rat endothelial cell antigen (RECA-1) antibody (1:25). (D, I,) Monoclonal α-Smooth Muscle – Cy3 antibody (1:400) (E,J) DAPI

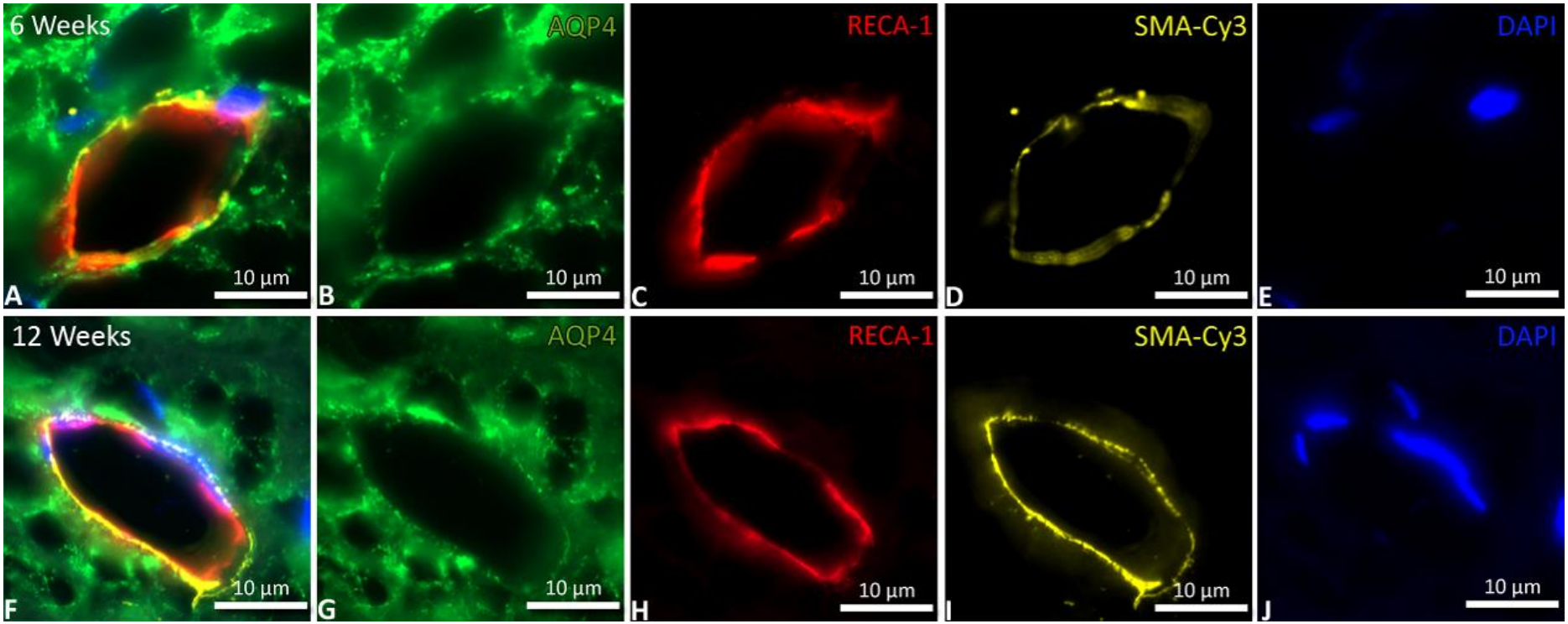

Figure 5. Examples of white matter arterioles in 6 and 12 week old rats. (A,F) A merged stack of all antibodies assessed at 630x resolution. (B,G) Polyclonal rabbit anti-rat AQP4 antibody (1:100). (C,H) Monoclonal mouse anti-rat endothelial cell antigen (RECA-1) antibody (1:25). (D, I,) Monoclonal α-Smooth Muscle – Cy3 antibody (1:400) (E,J) DAPI

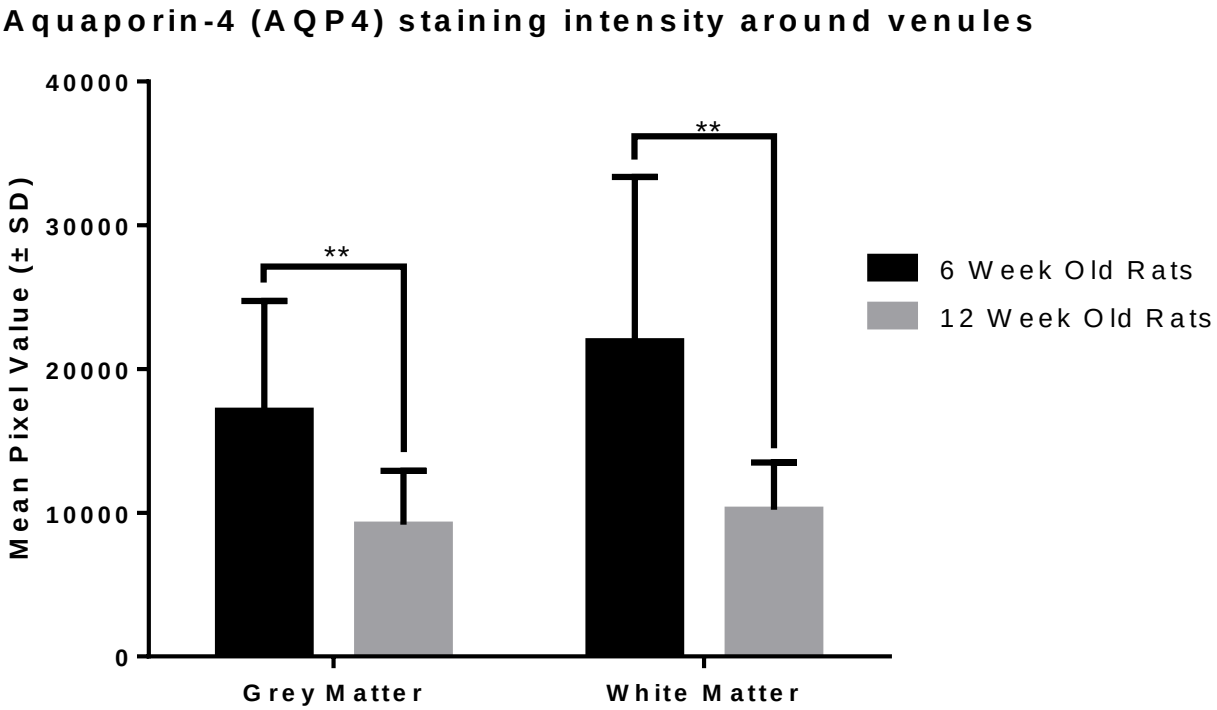

Figure 6. Calculated mean pixel values for aquaporin-4 staining around grey and white matter venules in 6 and 12 week old animals. Mean pixel intensity was determined using ImageJ software. Grey matter venules: 6 weeks n = 16, 12 weeks n = 20. White matter venules: 6 weeks n = 6, 12 weeks n = 13. ** = P <0.005. Error bars indicate ± SD

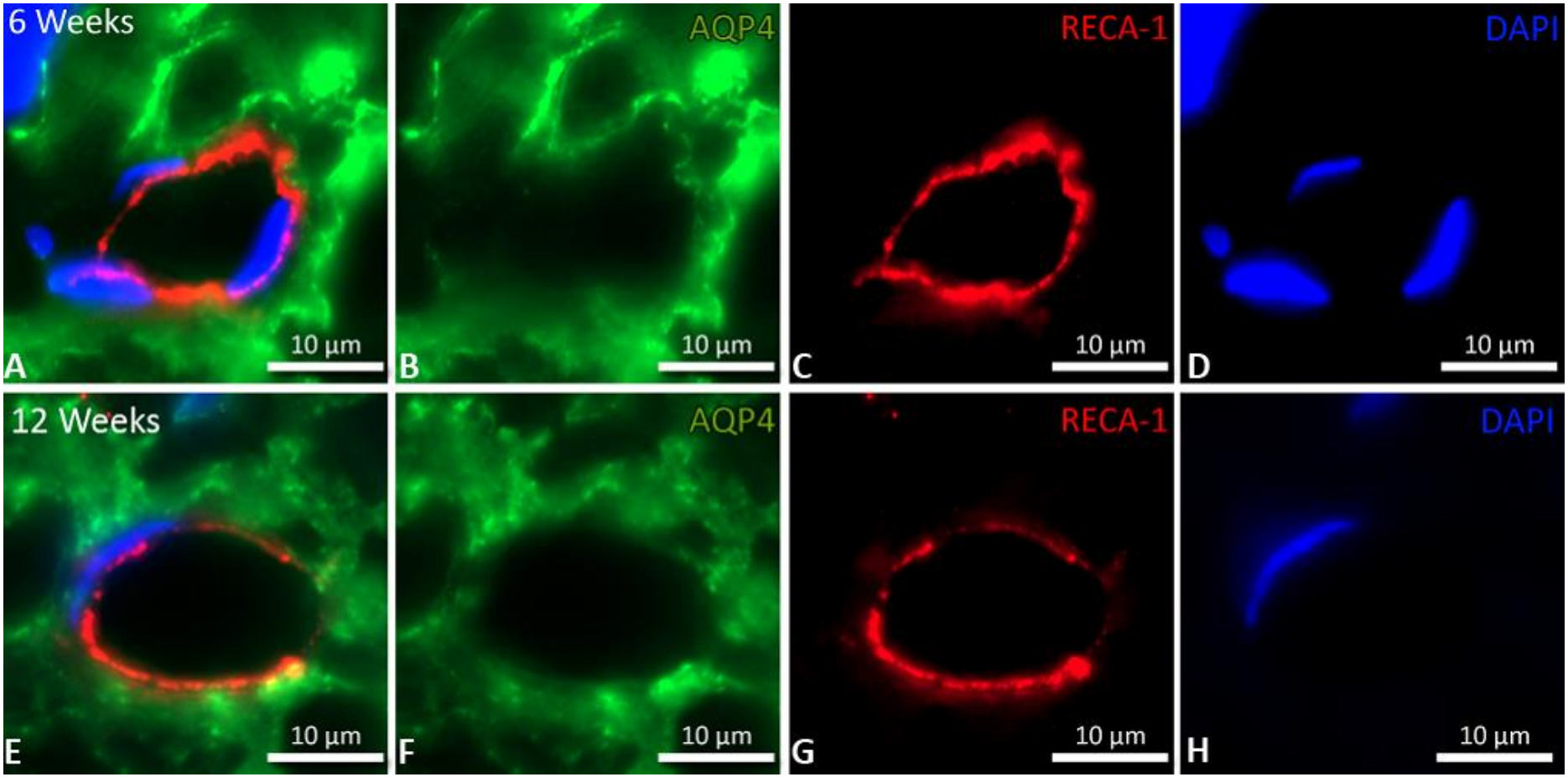

Figure 7. Examples of grey matter venules in 6 and 12 week old rats. (A,E) A merged stack of all antibodies assessed at 630x resolution. (B,F) Polyclonal rabbit anti-rat AQP4 antibody (1:100). (C,G) Monoclonal mouse anti-rat endothelial cell antigen (RECA-1) antibody (1:25). (D, H,) DAPI

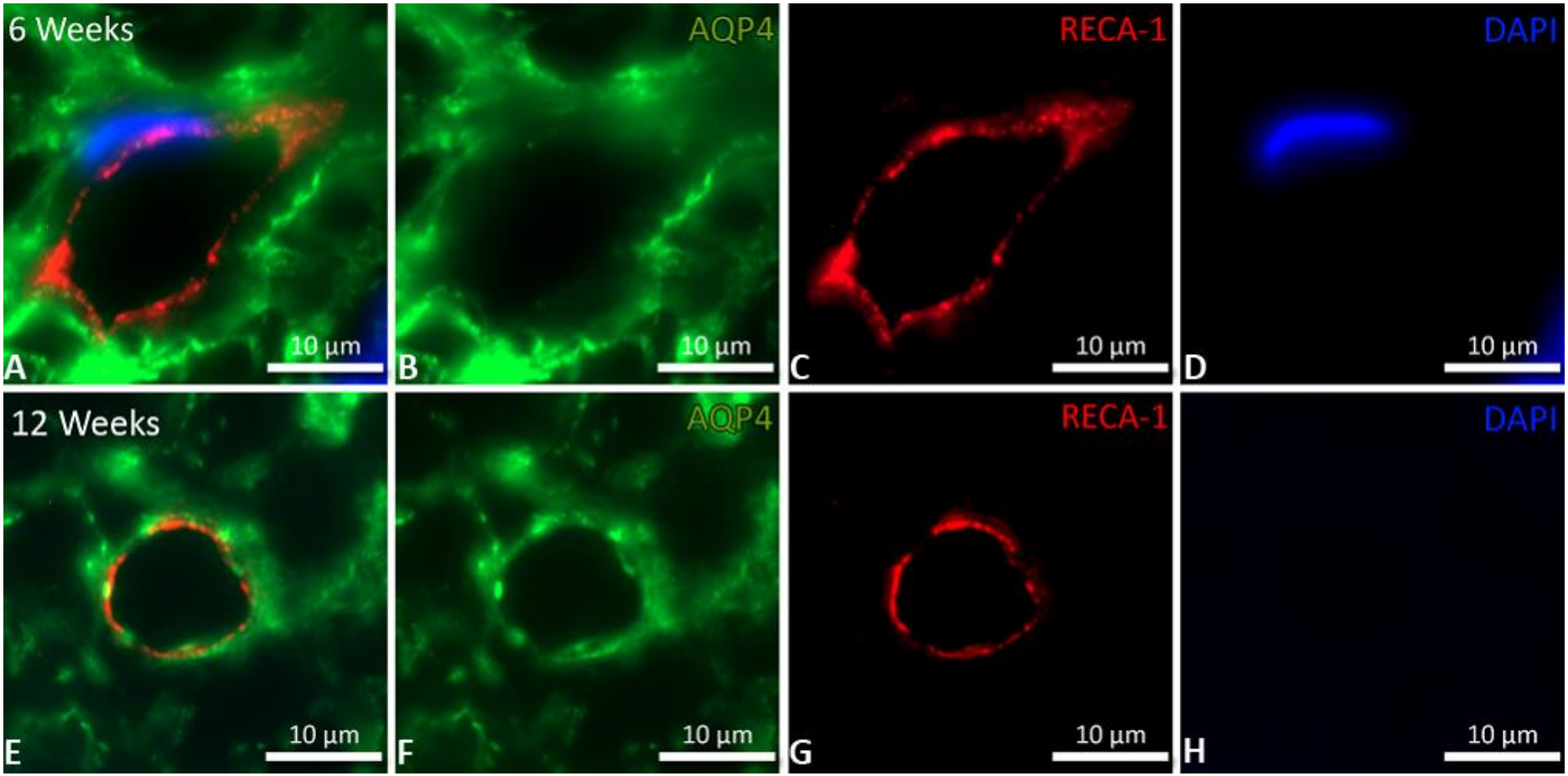

Figure 8. Examples of white matter venules in 6 and 12 week old rats. (A,E) A merged stack of all antibodies assessed at 630x resolution. (B,F) Polyclonal rabbit anti-rat AQP4 antibody (1:100). (C,G) Monoclonal mouse anti-rat endothelial cell antigen (RECA-1) antibody (1:25). (D, H,) DAPI

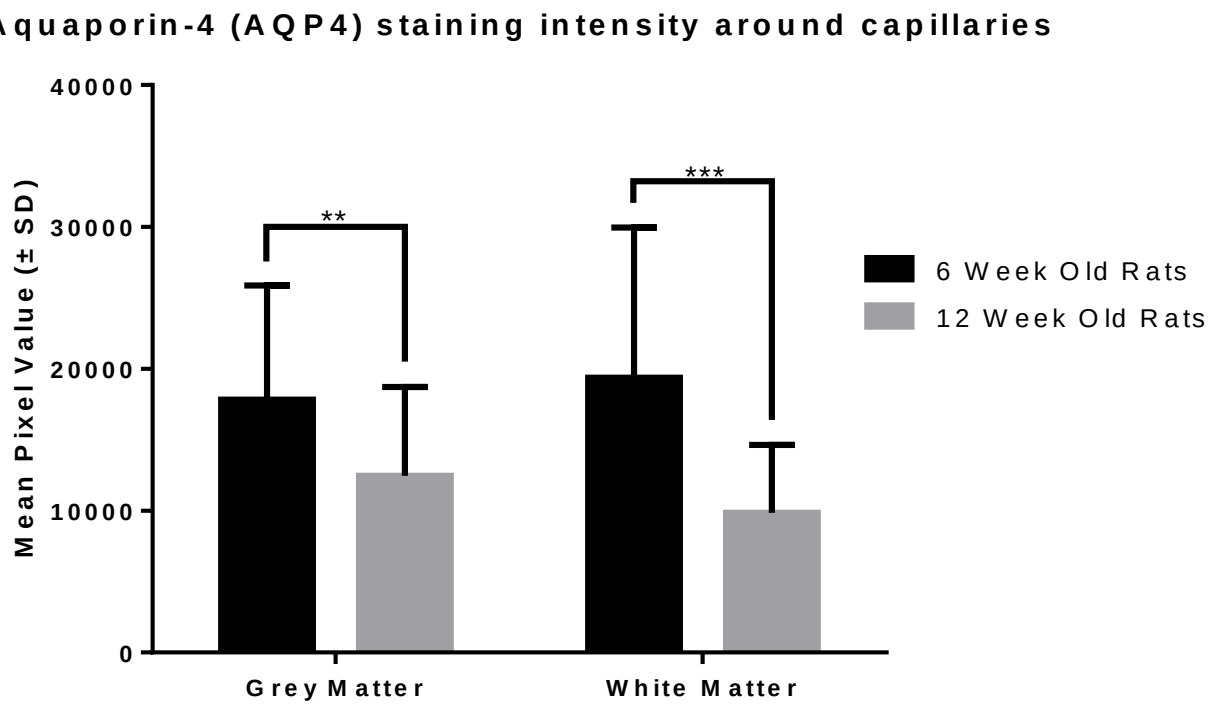

Figure 9. Calculated mean pixel values for aquaporin-4 staining around grey and white matter capillaries in 6 and 12 week old animals. Mean pixel intensity was determined using ImageJ software. Grey matter capillaries: 6 weeks n = 39, 12 weeks n = 42. White matter capillaries: 6 weeks n = 16, 12 weeks n = 25. ** = P <0.005, *** = P <0.0001. Error bars indicate ± SD

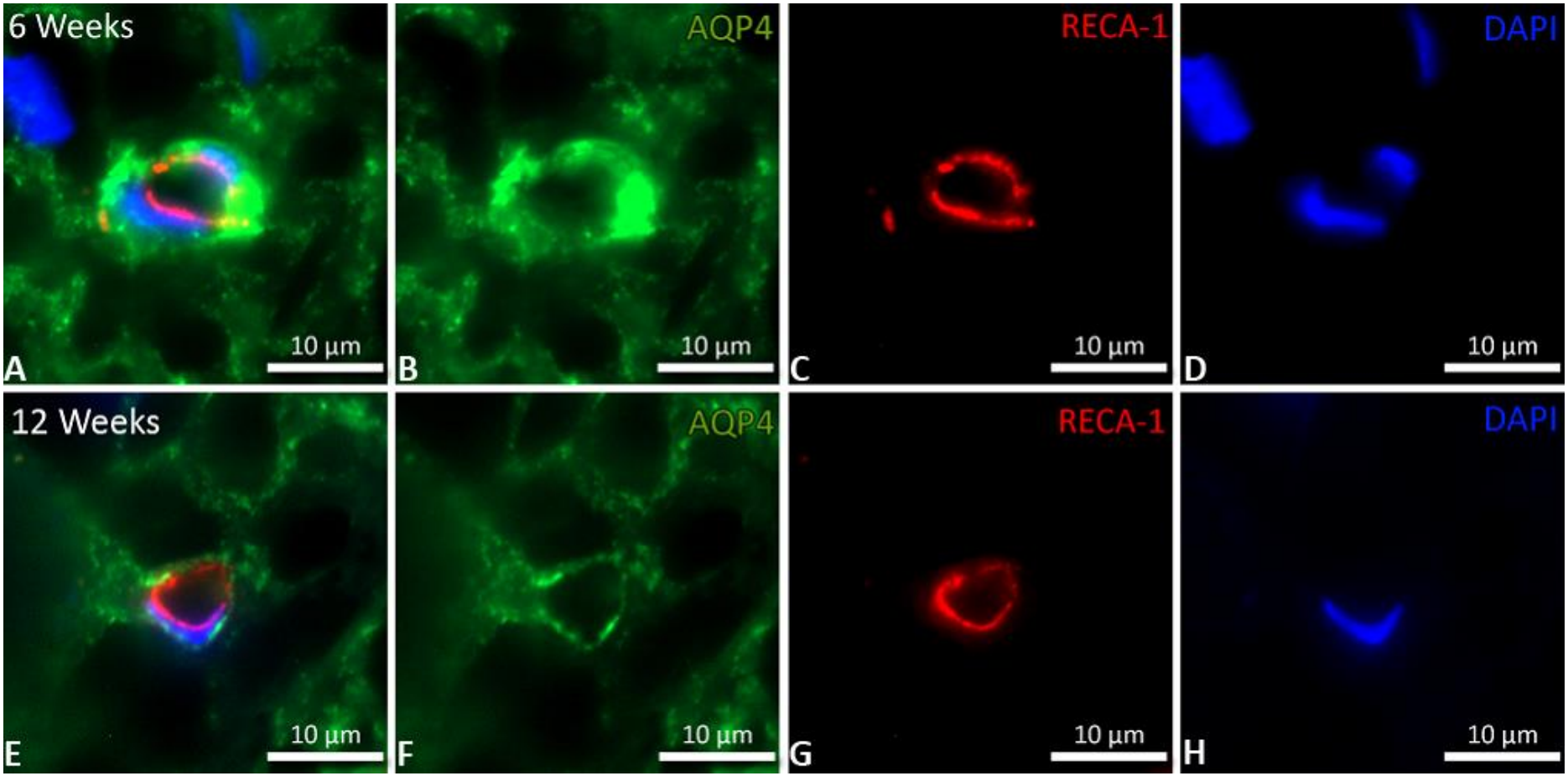

Figure 10. Examples of grey matter capillaries in 6 and 12 week old rats. (A,E) A merged stack of all antibodies assessed at 630x resolution. (B,F) Polyclonal rabbit anti-rat AQP4 antibody (1:100). (C,G) Monoclonal mouse anti-rat endothelial cell antigen (RECA-1) antibody (1:25). (D, H,) DAPI

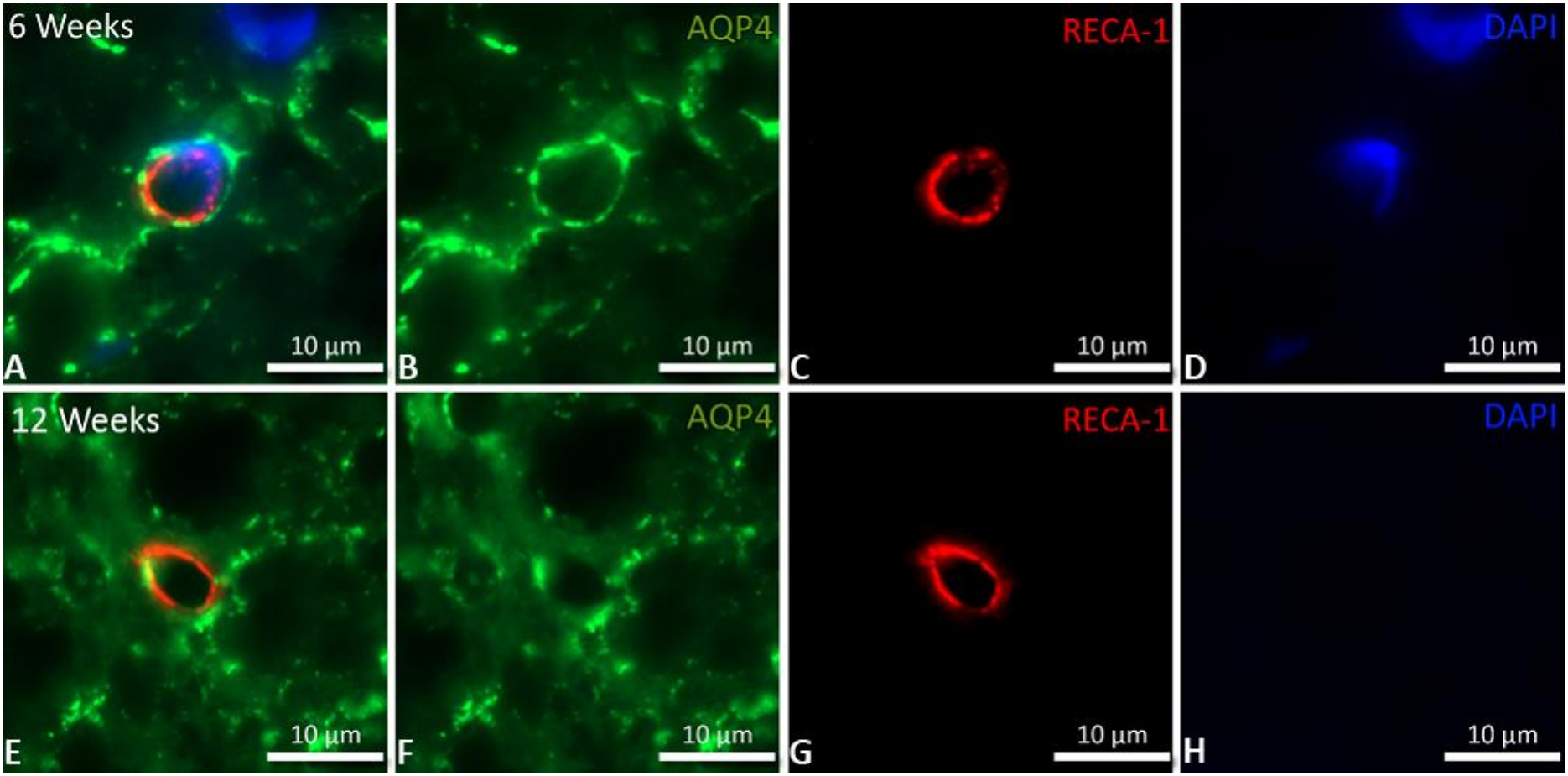

Figure 11. Examples of white matter capillaries for 6 and 12 week old rats. (A,E) A merged stack of all antibodies assessed at 630x resolution. (B,F) Polyclonal rabbit anti-rat AQP4 antibody (1:100). (C,G) Monoclonal mouse anti-rat endothelial cell antigen (RECA-1) antibody (1:25). (D, H,) DAPI

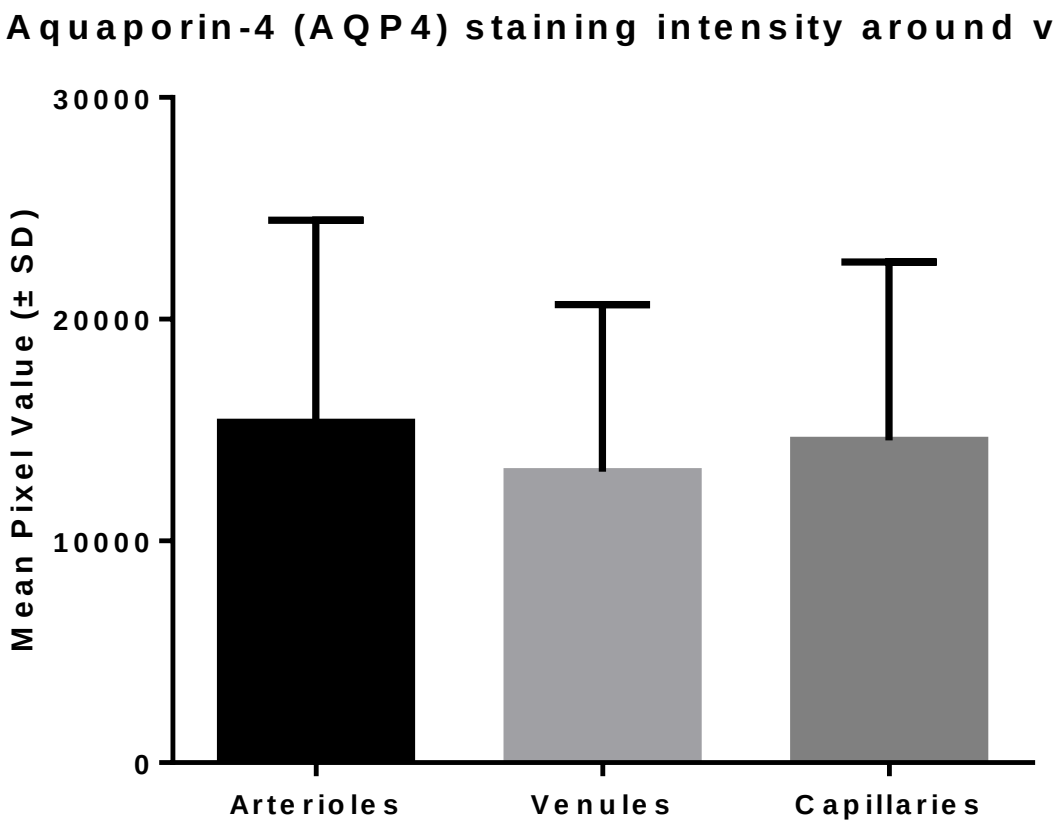

Figure 12. Calculated mean pixel intensities for aquaporin-4 staining around all arterioles, venules and capillaries that were analysed in this study. Mean Pixel Intensity was determined using ImageJ software. Arterioles: n = 125. Venules: n = 55, Capillaries: n = 122. Error bars indicate ± SD

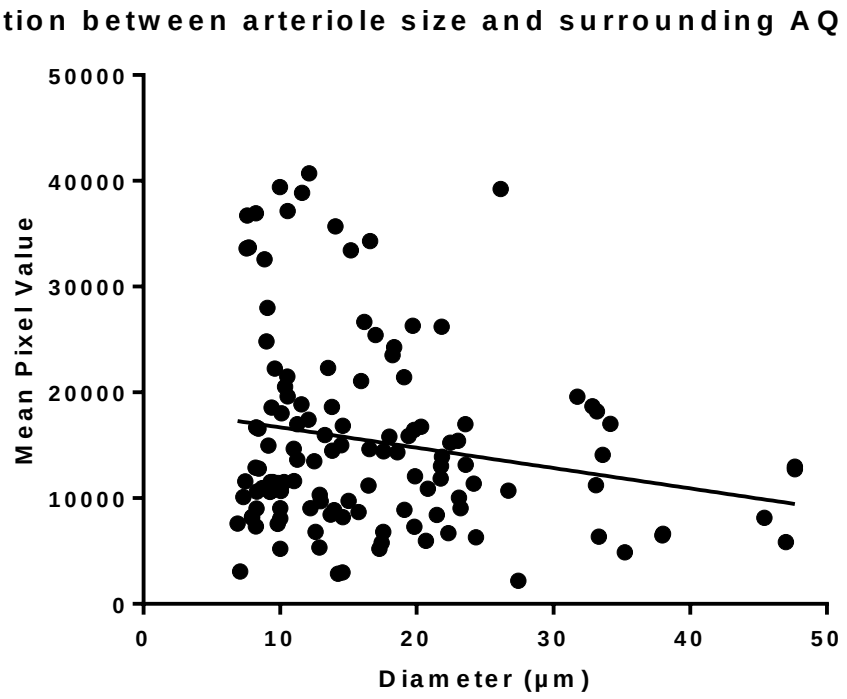

Figure 13. Correlations between the diameter of all arterioles studied and their mean pixel intensities. A statistically significant negative correlation was observed indicating that as the diameter of arterioles increases, the average amount of AQP4 surrounding them decreases.

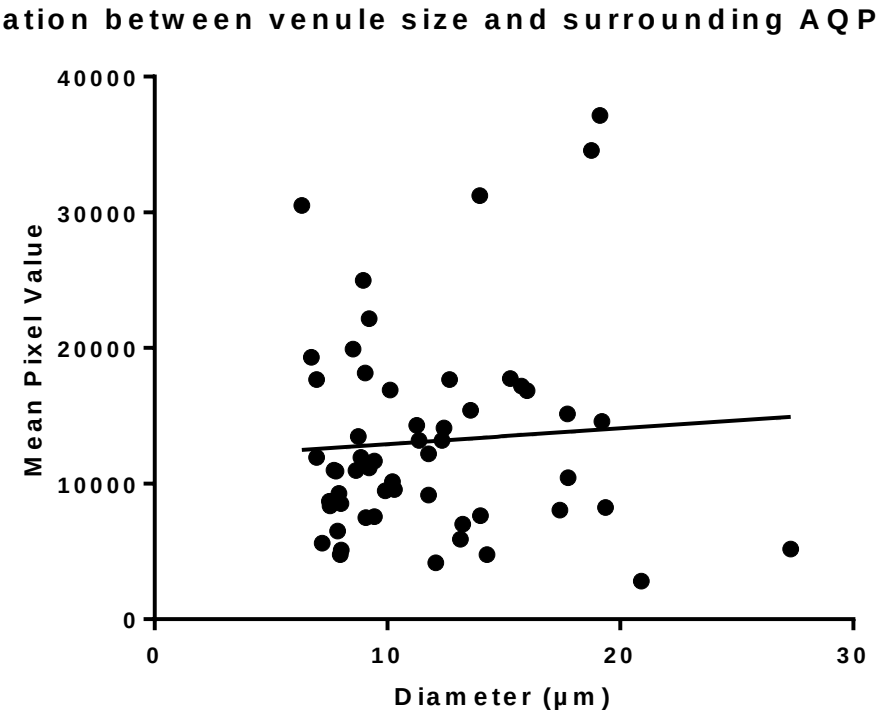

Figure 14. Correlations between the diameter of all venules studied and their mean pixel intensities. No significant correlations were observed between venule diameter and the average surrounding levels AQP4 expression.

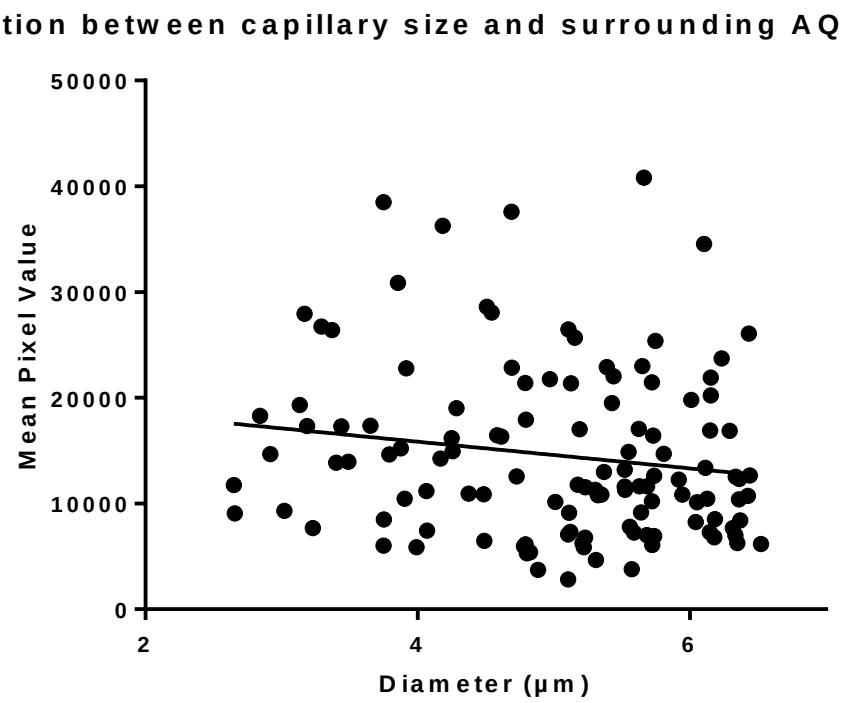

Figure 15. Correlations between the diameter of all capillaries studied and their mean pixel intensities. No significant correlations were observed between capillary diameter and the average surrounding levels AQP4 expression.

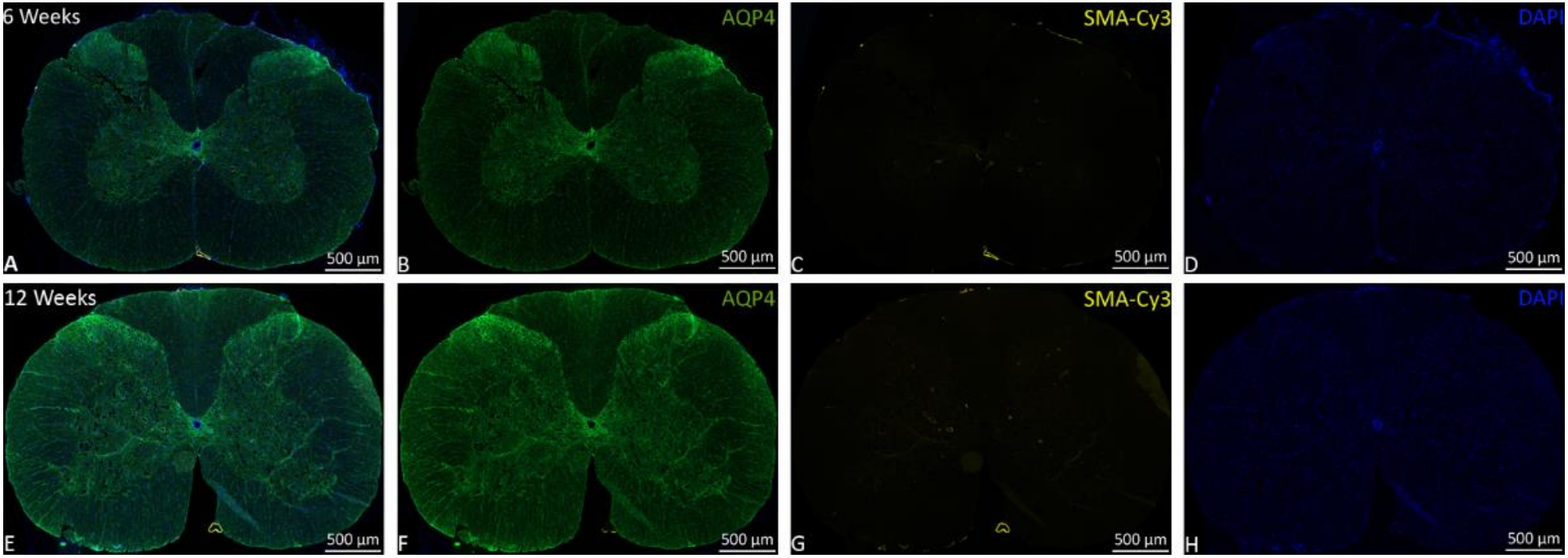

Figure 16. Examples of the overall pattern of aquaporin-4 expression observed in 6 and 12 week old rat spinal cords. (A,E) A merged stack of all antibodies assessed at 100x resolution. (B,F) Polyclonal rabbit anti-rat AQP4 antibody (1:100). (C,G) Monoclonal α-Smooth Muscle – Cy3 antibody (1:400) (D,H) DAPI

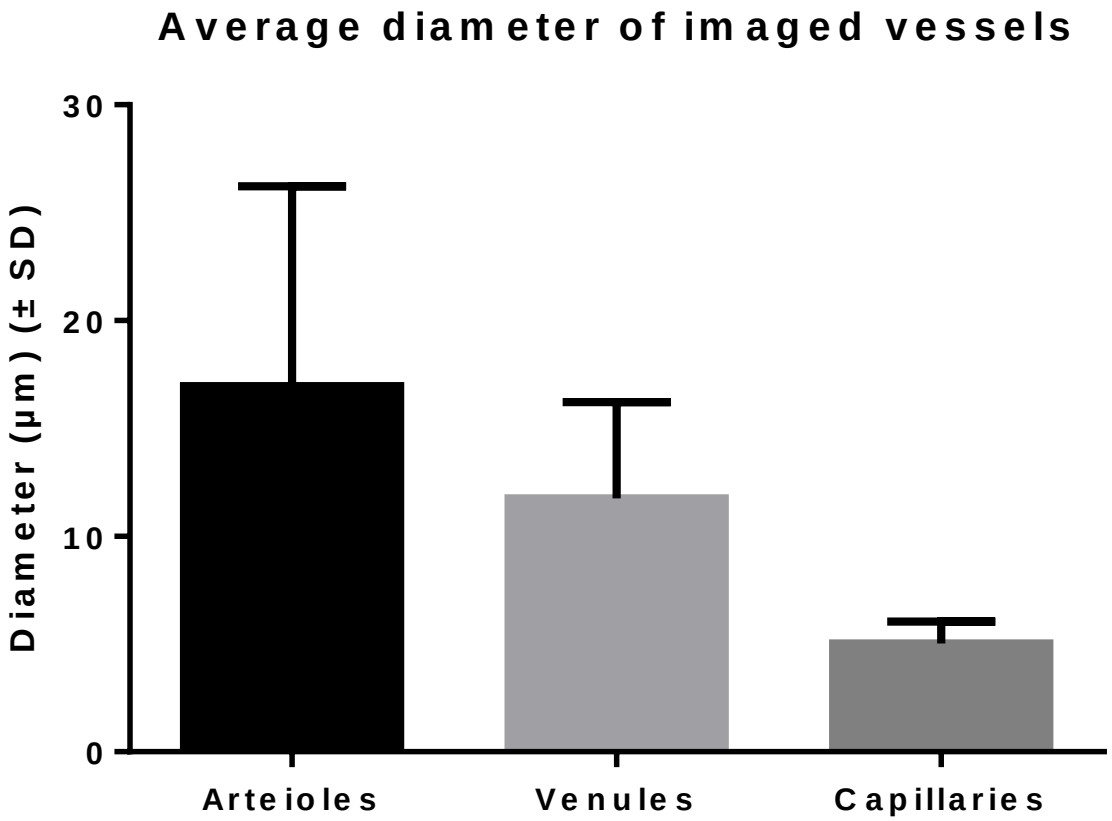

Figure 17. The average diameter calculated for all arterioles, venules and capillaries that were analysed in this study. Arterioles: n = 125. Venules: n =55. Capillaries: n = 122

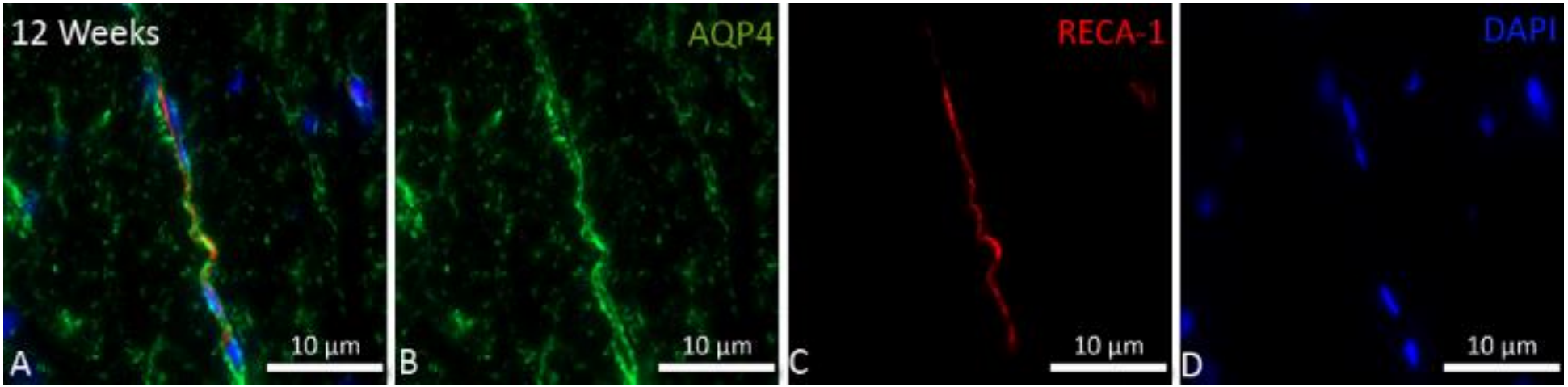

Figure 18. An example of an unidentified vessel located in the white matter of a 12 week old rat. As the diameter of this vessel could not be established, it was excluded from analysis in the study. It is important to note that a large amount of vessels in the white matter exhibited a similar pattern. This accounts for the low number of total white matter images analysed in comparison to grey matter.

References

Abbott, N.J. (2004). Evidence for bulk flow of brain interstitial fluid: significance for physiology and pathology. *Neurochem Int* 45**,** 545-552. doi: 10.1016/j.neuint.2003.11.006.

Aoki-Yoshino, K., Uchihara, T., Duyckaerts, C., Nakamura, A., Hauw, J.-J., and Wakayama, Y. (2005). Enhanced expression of aquaporin 4 in human brain with inflammatory diseases. *Acta Neuropathologica* 110**,** 281-288. doi: 10.1007/s00401-005-1052-2.

Badaut, J., Ashwal, S., Adami, A., Tone, B., Recker, R., Spagnoli, D., Ternon, B., and Obenaus, A. (2011). Brain water mobility decreases after astrocytic aquaporin-4 inhibition using RNA interference. *J Cereb Blood Flow Metab* 31**,** 819-831. doi: http://www.nature.com/jcbfm/journal/v31/n3/suppinfo/jcbfm2010163s1.html.

Badaut, J., Hirt, L., Granziera, C., Bogousslavsky, J., Magistretti, P.J., and Regli, L. (2001). Astrocyte-specific expression of aquaporin-9 in mouse brain is increased after transient focal cerebral ischemia. *J Cereb Blood Flow Metab* 21**,** 477-482. doi: 10.1097/00004647-200105000-00001.

Badaut, J., Petit, J.M., Brunet, J.F., Magistretti, P.J., Charriaut-Marlangue, C., and Regli, L. (2004). Distribution of Aquaporin 9 in the adult rat brain: preferential expression in catecholaminergic neurons and in glial cells. *Neuroscience* 128**,** 27-38. doi: 10.1016/j.neuroscience.2004.05.042.

Barkhof, F., Kouwenhoven, M., Scheltens, P., Sprenger, M., Algra, P., and Valk, J. (1994). Phase-contrast cine MR imaging of normal aqueductal CSF flow. Effect of aging and relation to CSF void on modulus MR. *Acta Radiol* 35**,** 123-130.

Bartanusz, V., Jezova, D., Alajajian, B., and Digicaylioglu, M. (2011). The blood-spinal cord barrier: morphology and clinical implications. *Ann Neurol* 70**,** 194-206. doi: 10.1002/ana.22421.

Battal, B., Kocaoglu, M., Bulakbasi, N., Husmen, G., Tuba Sanal, H., and Tayfun, C. (2011). Cerebrospinal fluid flow imaging by using phase-contrast MR technique. *Br J Radiol* 84**,** 758-765. doi: 10.1259/bjr/66206791.

Beck, S.T., Leite, O.M., Arruda, R.S., and Ferreira, A.W. (2005). Combined use of Western blot/ELISA to improve the serological diagnosis of human tuberculosis. *Braz J Infect Dis* 9**,** 35-43. doi: /S1413-86702005000100007.

Beckstead, J.H. (1994). A simple technique for preservation of fixation-sensitive antigens in paraffin-embedded tissues. *Journal of Histochemistry & Cytochemistry* 42**,** 1127-1134. doi: 10.1177/42.8.8027531.

Betsholtz, C. (2014). Physiology: Double function at the blood-brain barrier. *Nature* 509**,** 432-433. doi: 10.1038/nature13339.

Bulat, M., Lupret, V., Orehkovic, D., and Klarica, M. (2008). Transventricular and transpial absorption of cerebrospinal fluid into cerebral microvessels. *Coll Antropol* 32 Suppl 1**,** 43-50.

Castaneyra-Ruiz, L., Gonzalez-Marrero, I., Gonzalez-Toledo, J.M., Castaneyra-Ruiz, A., De Paz-Carmona, H., Castaneyra-Perdomo, A., and Carmona-Calero, E.M. (2013). Aquaporin-4 expression in the cerebrospinal fluid in congenital human hydrocephalus. *Fluids Barriers CNS* 10**,** 18. doi: 10.1186/2045-8118-10-18.

Charreau, B., Tesson, L., Soulillou, J.P., Pourcel, C., and Anegon, I. (1996). Transgenesis in rats: technical aspects and models. *Transgenic Res* 5**,** 223-234.

Chen, W., Song, X., and Zhang, Y. (2011). Assessment of the Virchow-Robin Spaces in Alzheimer disease, mild cognitive impairment, and normal aging, using high-field MR imaging. *AJNR Am J Neuroradiol* 32**,** 1490-1495. doi: 10.3174/ajnr.A2541.

Chikly, B., and Quaghebeur, J. (2013). Reassessing cerebrospinal fluid (CSF) hydrodynamics: A literature review presenting a novel hypothesis for CSF physiology. *Journal of Bodywork and Movement Therapies* 17**,** 344-354. doi: http://dx.doi.org/10.1016/j.jbmt.2013.02.002.

Corrales, J., and University, N.C.S. (2008). *Antimicrobial Polypeptides, Piscidins and Histone-like Proteins, in Important Aquacultured Fish and the Effect of Nutrition on Their Expression and Susceptibility to Infection in Hybrid Striped (sunshine) Bass (Morone Saxatilis X Morone Chrysops).* North Carolina State University.

Cottrell, J.E., and Young, W.L. (2010). *Cottrell and Young's Neuroanesthesia.* Elsevier Health Sciences.

Craven, J. (2010). Cerebrospinal fluid and its circulation. *Anaesthesia & Intensive Care Medicine* 11**,** 355-356. doi: http://dx.doi.org/10.1016/j.mpaic.2010.06.001.

Cserr, H.F., Harling-Berg, C.J., and Knopf, P.M. (1992). Drainage of brain extracellular fluid into blood and deep cervical lymph and its immunological significance. *Brain Pathol* 2**,** 269-276.

Do Carmo, S., and Cuello, A.C. (2013). Modeling Alzheimer's disease in transgenic rats. *Mol Neurodegener* 8**,** 37. doi: 10.1186/1750-1326-8-37.

Dore-Duffy, P. (2008). Pericytes: pluripotent cells of the blood brain barrier. *Curr Pharm Des* 14**,** 1581-1593.

Ducker, T.B., and Hamit, H.F. (1969). Experimental treatments of acute spinal cord injury. *Journal of neurosurgery* 30**,** 693-697.

Edsbagge, M., Starck, G., Zetterberg, H., Ziegelitz, D., and Wikkelso, C. (2011). Spinal cerebrospinal fluid volume in healthy elderly individuals. *Clinical Anatomy* 24**,** 733-740. doi: 10.1002/ca.21153.

Enzmann, D.R., and Pelc, N.J. (1992). Brain motion: measurement with phase-contrast MR imaging. *Radiology* 185**,** 653-660. doi: 10.1148/radiology.185.3.1438741.

Esiri, M.M., and Gay, D. (1990). Immunological and neuropathological significance of the Virchow-Robin space. *J Neurol Sci* 100**,** 3-8.

Etemadifar, M., Hekmatnia, A., Tayari, N., Kazemi, M., Ghazavi, A., Akbari, M., and Maghzi, A.H. (2011). Features of Virchow-Robin spaces in newly diagnosed multiple sclerosis patients. *Eur J Radiol* 80**,** e104-108. doi: 10.1016/j.ejrad.2010.05.018.

Gallagher, S., and Chakavarti, D. (2008). Immunoblot analysis. *J Vis Exp*. doi: 10.3791/759.

Ge, S., and Pachter, J.S. (2006). Isolation and culture of microvascular endothelial cells from murine spinal cord. *Journal of Neuroimmunology* 177**,** 209-214. doi: http://dx.doi.org/10.1016/j.jneuroim.2006.05.012.

Ghersi-Egea, J.F., Finnegan, W., Chen, J.L., and Fenstermacher, J.D. (1996). Rapid distribution of intraventricularly administered sucrose into cerebrospinal fluid cisterns via subarachnoid velae in rat. *Neuroscience* 75**,** 1271-1288.

Goswami, J.M., S.; Mondal, A.; Ganguly, S.; Paul, I.; Mukhopadhayay S. K. (2012). Immunohistochemistry: a novel tool for the diagnosis of animal disease. *International Journal of Bio-resource and Stress Management* 3**,** 109-115.

Greitz, D. (1993). Cerebrospinal fluid circulation and associated intracranial dynamics. A radiologic investigation using MR imaging and radionuclide cisternography. *Acta Radiol Suppl* 386**,** 1-23.

Groeschel, S., Chong, W.K., Surtees, R., and Hanefeld, F. (2006). Virchow-Robin spaces on magnetic resonance images: normative data, their dilatation, and a review of the literature. *Neuroradiology* 48**,** 745-754. doi: 10.1007/s00234-006-0112-1.

Gupta, R.K., and Kanungo, M. (2013). Glial molecular alterations with mouse brain development and aging: up-regulation of the Kir4.1 and aquaporin-4. *Age (Dordr)* 35**,** 59-67. doi: 10.1007/s11357-011-9330-5.

Gupta, S., Soellinger, M., Grzybowski, D.M., Boesiger, P., Biddiscombe, J., Poulikakos, D., and Kurtcuoglu, V. (2010). Cerebrospinal fluid dynamics in the human cranial subarachnoid space: an overlooked mediator of cerebral disease. I. Computational model. *J R Soc Interface* 7**,** 1195-1204. doi: 10.1098/rsif.2010.0033.

Hashizume, Y., Yasui, K., and Yoshida, M. (2001). "Age-Related Morphological Change of the Central Canal of the Human Spinal Cord and the Mechanism of Syrinx Formation in Syringomyelia and Hydromyelia," in *Syringomyelia,* eds. N. Tamaki, U. Batzdorf & T. Nagashima. Springer Japan), 31-39.

Heidebrecht, F., Heidebrecht, A., Schulz, I., Behrens, S.E., and Bader, A. (2009). Improved semiquantitative Western blot technique with increased quantification range. *Journal of Immunological Methods* 345**,** 40-48. doi: http://dx.doi.org/10.1016/j.jim.2009.03.018.

Hemley, S.J., Bilston, L.E., Cheng, S., Chan, J.N., and Stoodley, M.A. (2013). Aquaporin-4 expression in post-traumatic syringomyelia. *J Neurotrauma* 30**,** 1457-1467. doi: 10.1089/neu.2012.2614.

Hemley, S.J., Bilston, L.E., Cheng, S., and Stoodley, M.A. (2012). Aquaporin-4 expression and blood–spinal cord barrier permeability in canalicular syringomyelia. *Journal of Neurosurgery: Spine* 17**,** 602-612. doi: doi:10.3171/2012.9.SPINE1265.

Hogan, Q.H., Prost, R., Kulier, A., Taylor, M.L., Liu, S., and Mark, L. (1996). Magnetic resonance imaging of cerebrospinal fluid volume and the influence of body habitus and abdominal pressure. *Anesthesiology* 84**,** 1341-1349.

Huang, P., Duda, D.G., Jain, R.K., and Fukumura, D. (2008). Histopathologic findings and establishment of novel tumor lines from spontaneous tumors in FVB/N mice. *Comp Med* 58**,** 253-263.

Ichimura, T., Fraser, P.A., and Cserr, H.F. (1991). Distribution of extracellular tracers in perivascular spaces of the rat brain. *Brain Res* 545**,** 103-113.

Iliff, J.J., and Nedergaard, M. (2013). Is there a cerebral lymphatic system? *Stroke* 44**,** S93-95. doi: 10.1161/strokeaha.112.678698.

Iliff, J.J., Wang, M., Liao, Y., Plogg, B.A., Peng, W., Gundersen, G.A., Benveniste, H., Vates, G.E., Deane, R., Goldman, S.A., Nagelhus, E.A., and Nedergaard, M. (2012). A paravascular pathway facilitates CSF flow through the brain parenchyma and the clearance of interstitial solutes, including amyloid beta. *Sci Transl Med* 4**,** 147ra111. doi: 10.1126/scitranslmed.3003748.

Iliff, J.J., Wang, M., Zeppenfeld, D.M., Venkataraman, A., Plog, B.A., Liao, Y., Deane, R., and Nedergaard, M. (2013). Cerebral arterial pulsation drives paravascular CSF-interstitial fluid exchange in the murine brain. *J Neurosci* 33**,** 18190-18199. doi: 10.1523/jneurosci.1592-13.2013.

Jarius, S., Franciotta, D., Paul, F., Bergamaschi, R., Rommer, P.S., Ruprecht, K., Ringelstein, M., Aktas, O., Kristoferitsch, W., and Wildemann, B. (2012). Testing for antibodies to human aquaporin-4 by ELISA: Sensitivity, specificity, and direct comparison with immunohistochemistry. *Journal of the Neurological Sciences* 320**,** 32-37. doi: http://dx.doi.org/10.1016/j.jns.2012.06.002.

Jeong, J.H., Sugii, Y., Minamiyama, M., and Okamoto, K. (2006). Measurement of RBC deformation and velocity in capillaries in vivo. *Microvasc Res* 71**,** 212-217. doi: 10.1016/j.mvr.2006.02.006.

Johanson, C.E., Duncan, J.A., 3rd, Klinge, P.M., Brinker, T., Stopa, E.G., and Silverberg, G.D. (2008). Multiplicity of cerebrospinal fluid functions: New challenges in health and disease. *Cerebrospinal Fluid Res* 5**,** 10. doi: 10.1186/1743-8454-5-10.

Jones, C.J.H., Kuo, L., Davis, M.J., Defily, D.V., and Chilian, W.M. (1995). Role of Nitric Oxide in the Coronary Microvascular Responses to Adenosine and Increased Metabolic Demand. *Circulation* 91**,** 1807-1813. doi: 10.1161/01.cir.91.6.1807.

Killer, H.E., Jaggi, G.P., Flammer, J., Miller, N.R., Huber, A.R., and Mironov, A. (2007). Cerebrospinal fluid dynamics between the intracranial and the subarachnoid space of the optic nerve. Is it always bidirectional? *Brain* 130**,** 514-520. doi: 10.1093/brain/awl324.

Kundi, S., R. Bicknell and Z. Ahmed (2013). Spinal cord injury : current mammalian models. *Am. J. Neurosci* 4**,** 1-12. doi: 10.3844/amjnsp.2013.1.12.

Laterra, J.K., R. Betz, L. Goldstein, G. (1999). "Blood—Cerebrospinal Fluid Barrier," in *Basic Neurochemistry: Molecular, Cellular and Medical Aspects,* eds. S. Brady, G. Siegel, R.W. Albers & D. Price. 6 ed: Elsevier Science).

Lee, J.S., Semela, D., Iredale, J., and Shah, V.H. (2007). Sinusoidal remodeling and angiogenesis: a new function for the liver-specific pericyte? *Hepatology* 45**,** 817-825. doi: 10.1002/hep.21564.

Longatti, P.L., Basaldella, L., Orvieto, E., Fiorindi, A., and Carteri, A. (2004). Choroid plexus and aquaporin-1: A novel explanation of cerebrospinal fluid production. *Pediatric Neurosurgery* 40**,** 277-283.

Lu, H., Lei, X.Y., Hu, H., and He, Z.P. (2013). Relationship between AQP4 expression and structural damage to the blood-brain barrier at early stages of traumatic brain injury in rats. *Chin Med J (Engl)* 126**,** 4316-4321.

Mahmood, T., and Yang, P.C. (2012). Western blot: technique, theory, and trouble shooting. *N Am J Med Sci* 4**,** 429-434. doi: 10.4103/1947-2714.100998.

Milhorat, T.H., Kotzen, R.M., and Anzil, A.P. (1994). Stenosis of central canal of spinal cord in man: incidence and pathological findings in 232 autopsy cases. *J Neurosurg* 80**,** 716-722. doi: 10.3171/jns.1994.80.4.0716.

Milhorat, T.N., S. Heger, I. Nobandegani, F. Murray S. (1992). Ultrastructural evidence of sink function of central canal of spinal cord as demonstated by clearance of horseradish peroxidase. *Proc Electron Micros Soc Am* 50**,** 700-701.

Misu, T., Fujihara, K., Kakita, A., Konno, H., Nakamura, M., Watanabe, S., Takahashi, T., Nakashima, I., Takahashi, H., and Itoyama, Y. (2007). Loss of aquaporin 4 in lesions of neuromyelitis optica: distinction from multiple sclerosis. *Brain* 130**,** 1224-1234. doi: 10.1093/brain/awm047.

Mobasheri, A., Marples, D., Young, I.S., Floyd, R.V., Moskaluk, C.A., and Frigeri, A. (2007). Distribution of the AQP4 water channel in normal human tissues: protein and tissue microarrays reveal expression in several new anatomical locations, including the prostate gland and seminal vesicles. *Channels (Austin)* 1**,** 29-38.

Morikawa, S., Baluk, P., Kaidoh, T., Haskell, A., Jain, R.K., and Mcdonald, D.M. (2002). Abnormalities in pericytes on blood vessels and endothelial sprouts in tumors. *Am J Pathol* 160**,** 985-1000. doi: 10.1016/s0002-9440(10)64920-6.

Muthukumar, N. (2012). Syringomyelia as a presenting feature of shunt dysfunction: Implications for the pathogenesis of syringomyelia. *J Craniovertebr Junction Spine* 3**,** 26-31. doi: 10.4103/0974-8237.110125.

Nehls, V., and Drenckhahn, D. (1993). The versatility of microvascular pericytes: from mesenchyme to smooth muscle? *Histochemistry* 99**,** 1-12. doi: 10.1007/BF00268014.

Nesic, O., Guest, J.D., Zivadinovic, D., Narayana, P.A., Herrera, J.J., Grill, R.J., Mokkapati, V.U., Gelman, B.B., and Lee, J. (2010). Aquaporins in spinal cord injury: the janus face of aquaporin 4. *Neuroscience* 168**,** 1019-1035. doi: 10.1016/j.neuroscience.2010.01.037.

Nesic, O., Lee, J., Unabia, G.C., Johnson, K., Ye, Z., Vergara, L., Hulsebosch, C.E., and Perez-Polo, J.R. (2008). Aquaporin 1 - a novel player in spinal cord injury. *J Neurochem* 105**,** 628-640. doi: 10.1111/j.1471-4159.2007.05177.x.

Nesic, O., Lee, J., Ye, Z., Unabia, G.C., Rafati, D., Hulsebosch, C.E., and Perez-Polo, J.R. (2006). Acute and chronic changes in aquaporin 4 expression after spinal cord injury. *Neuroscience* 143**,** 779-792. doi: 10.1016/j.neuroscience.2006.08.079.

Nicchia, G.P., Nico, B., Camassa, L.M., Mola, M.G., Loh, N., Dermietzel, R., Spray, D.C., Svelto, M., and Frigeri, A. (2004). The role of aquaporin-4 in the blood-brain barrier development and integrity: studies in animal and cell culture models. *Neuroscience* 129**,** 935-945. doi: 10.1016/j.neuroscience.2004.07.055.

Nico, B., Frigeri, A., Nicchia, G.P., Quondamatteo, F., Herken, R., Errede, M., Ribatti, D., Svelto, M., and Roncali, L. (2001). Role of aquaporin-4 water channel in the development and integrity of the blood-brain barrier. *Journal of Cell Science* 114**,** 1297-1307.

Nielsen, S., Nagelhus, E.A., Amiry-Moghaddam, M., Bourque, C., Agre, P., and Ottersen, O.P. (1997). Specialized membrane domains for water transport in glial cells: high-resolution immunogold cytochemistry of aquaporin-4 in rat brain. *J Neurosci* 17**,** 171-180.

Nilsson, C., Lindvall-Axelsson, M., and Owman, C. (1992). Neuroendocrine regulatory mechanisms in the choroid plexus-cerebrospinal fluid system. *Brain Res Brain Res Rev* 17**,** 109-138.

Noell, S., Fallier-Becker, P., Deutsch, U., Mack, A., and Wolburg, H. (2009). Agrin defines polarized distribution of orthogonal arrays of particles in astrocytes. *Cell and Tissue Research* 337**,** 185-195. doi: 10.1007/s00441-009-0812-z.

Obermeier, B., Daneman, R., and Ransohoff, R.M. (2013). Development, maintenance and disruption of the blood-brain barrier. *Nat Med* 19**,** 1584-1596. doi: 10.1038/nm.3407.

Oklinski, M.K., Lim, J.S., Choi, H.J., Oklinska, P., Skowronski, M.T., and Kwon, T.H. (2014). Immunolocalization of Water Channel Proteins AQP1 and AQP4 in Rat Spinal Cord. *J Histochem Cytochem* 62**,** 598-611. doi: 10.1369/0022155414537495.

Oshio, K., Binder, D.K., Yang, B., Schecter, S., Verkman, A.S., and Manley, G.T. (2004). Expression of aquaporin water channels in mouse spinal cord. *Neuroscience* 127**,** 685-693. doi: 10.1016/j.neuroscience.2004.03.016.

Oshio, K., Song, Y., Verkman, A.S., and Manley, G.T. (2003). Aquaporin-1 deletion reduces osmotic water permeability and cerebrospinal fluid production. *Acta neurochirurgica. Supplement* 86**,** 525-528.

Oshio, K., Watanabe, H., Song, Y., Verkman, A.S., and Manley, G.T. (2005). Reduced cerebrospinal fluid production and intracranial pressure in mice lacking choroid plexus water channel Aquaporin-1. *Faseb j* 19**,** 76-78. doi: 10.1096/fj.04-1711fje.

Owler, B.K., Pitham, T., and Wang, D. (2010). Aquaporins: relevance to cerebrospinal fluid physiology and therapeutic potential in hydrocephalus. *Cerebrospinal Fluid Res* 7**,** 15. doi: 10.1186/1743-8454-7-15.

Pan, W., Banks, W.A., and Kastin, A.J. (1997). Permeability of the blood–brain and blood–spinal cord barriers to interferons. *Journal of Neuroimmunology* 76**,** 105-111. doi: http://dx.doi.org/10.1016/S0165-5728(97)00034-9.

Papadopoulos, M.C., and Verkman, A.S. (2005). Aquaporin-4 gene disruption in mice reduces brain swelling and mortality in pneumococcal meningitis. *J Biol Chem* 280**,** 13906-13912. doi: 10.1074/jbc.M413627200.

Park, E., Bell, J.D., Siddiq, I.P., and Baker, A.J. (2008). An analysis of regional microvascular loss and recovery following two grades of fluid percussion trauma: a

role for hypoxia-inducible factors in traumatic brain injury. *J Cereb Blood Flow Metab* 29**,** 575-584.
Potokar, M., Stenovec, M., Jorgacevski, J., Holen, T., Kreft, M., Ottersen, O.P., and Zorec, R. (2013). Regulation of AQP4 surface expression via vesicle mobility in astrocytes. *Glia* 61**,** 917-928. doi: 10.1002/glia.22485.
Quaia, E., and Bartolotta, T.V. (2005). *Contrast Media in Ultrasonography: Basic Principles and Clinical Applications.* Springer.
Rash, J.E., Yasumura, T., Hudson, C.S., Agre, P., and Nielsen, S. (1998). Direct immunogold labeling of aquaporin-4 in square arrays of astrocyte and ependymocyte plasma membranes in rat brain and spinal cord. *Proc Natl Acad Sci U S A* 95**,** 11981-11986.
Redzic, Z. (2011). Molecular biology of the blood-brain and the blood-cerebrospinal fluid barriers: similarities and differences. *Fluids Barriers CNS* 8**,** 3. doi: 10.1186/2045-8118-8-3.
Rennels, M.L., Gregory, T.F., Blaumanis, O.R., Fujimoto, K., and Grady, P.A. (1985). Evidence for a 'Paravascular' fluid circulation in the mammalian central nervous system, provided by the rapid distribution of tracer protein throughout the brain from the subarachnoid space. *Brain Research* 326**,** 47-63. doi: http://dx.doi.org/10.1016/0006-8993(85)91383-6.
Rhodin, J.a.G. (1967). The ultrastructure of mammalian arterioles and precapillary sphincters. *Journal of Ultrastructure Research* 18**,** 181-223. doi: http://dx.doi.org/10.1016/S0022-5320(67)80239-9.
Rizvi, S.A., and Coyle, P.K. (2011). *Clinical Neuroimmunology: Multiple Sclerosis and Related Disorders.* Humana Press.
Robin, C. (1859). Recherches sur quelques particularités de la structure des capillaires de l'encephale. *J Physiol Homme Anim* 2**,** 537-548.
Roncali, L., Nico, B., Ribatti, D., Bertossi, M., and Mancini, L. (1986). Microscopical and ultrastructural investigations on the development of the blood-brain barrier in the chick embryo optic tectum. *Acta Neuropathologica* 70**,** 193-201.
Saadoun, S., Bell, B.A., Verkman, A.S., and Papadopoulos, M.C. (2008). Greatly improved neurological outcome after spinal cord compression injury in AQP4-deficient mice. *Brain* 131**,** 1087-1098. doi: 10.1093/brain/awn014.
Satoh, J., Tabunoki, H., Yamamura, T., Arima, K., and Konno, H. (2007). Human astrocytes express aquaporin-1 and aquaporin-4 in vitro and in vivo. *Neuropathology* 27**,** 245-256.
Saubamea, B., Cochois-Guegan, V., Cisternino, S., and Scherrmann, J.-M. (2012). Heterogeneity in the rat brain vasculature revealed by quantitative confocal analysis of endothelial barrier antigen and P-glycoprotein expression. *J Cereb Blood Flow Metab* 32**,** 81-92.
Schulze, C., and Firth, J.A. (1992). Interendothelial junctions during blood-brain barrier development in the rat: Moprhological changes at the level of individual tight junctional contacts. *Developmental Brain Research* 69**,** 85-95.
Sharma, H.S., and Olsson, Y. (1990). Edema formation and cellular alterations following spinal cord injury in the rat and their modification with p-chlorophenylalanine. *Acta Neuropathol* 79**,** 604-610.
Shepard, M.J., and Bracken, M.B. (1999). Magnetic resonance imaging and neurological recovery in acute spinal cord injury: observations from the National Acute Spinal Cord Injury Study 3. *Spinal Cord* 37**,** 833-837.
Shi, S.R., Shi, Y., and Taylor, C.R. (2011). Antigen retrieval immunohistochemistry: review and future prospects in research and diagnosis over two decades. *J Histochem Cytochem* 59**,** 13-32. doi: 10.1369/jhc.2010.957191.

Shields, S.D., Mazario, J., Skinner, K., and Basbaum, A.I. (2007). Anatomical and functional analysis of aquaporin 1, a water channel in primary afferent neurons. *Pain* 131**,** 8-20. doi: 10.1016/j.pain.2006.11.018.

Shiraishi, T., Sakaki, S., and Uehara, Y. (1990). Architecture of the medial smooth muscle of the arterial vessels in the normal human brain: a scanning electron-microscopic study. *Scanning Microsc* 4**,** 191-199; discussion 199.

Skalli, O., Pelte, M.F., Peclet, M.C., Gabbiani, G., Gugliotta, P., Bussolati, G., Ravazzola, M., and Orci, L. (1989). Alpha-smooth muscle actin, a differentiation marker of smooth muscle cells, is present in microfilamentous bundles of pericytes. *J Histochem Cytochem* 37**,** 315-321.

So, P.T.C. (2001). "Two-photon Fluorescence Light Microscopy," in *eLS*. John Wiley & Sons, Ltd).

Speake, T., Freeman, L.J., and Brown, P.D. (2003). Expression of aquaporin 1 and aquaporin 4 water channels in rat choroid plexus. *Biochimica et Biophysica Acta (BBA) - Biomembranes* 1609**,** 80-86. doi: http://dx.doi.org/10.1016/S0005-2736(02)00658-2.

Stoodley, M.A., Brown, S.A., Brown, C.J., and Jones, N.R. (1997). Arterial pulsation-dependent perivascular cerebrospinal fluid flow into the central canal in the sheep spinal cord. *J Neurosurg* 86**,** 686-693. doi: 10.3171/jns.1997.86.4.0686.

Stoodley, M.A., Jones, N.R., and Brown, C.J. (1996). Evidence for rapid fluid flow from the subarachnoid space into the spinal cord central canal in the rat. *Brain Res* 707**,** 155-164.

Stover, J.F., Pleines, U.E., Morganti-Kossmann, M.C., Kossmann, T., Lowitzsch, K., and Kempski, O.S. (1997). Neurotransmitters in cerebrospinal fluid reflect pathological activity. *Eur J Clin Invest* 27**,** 1038-1043.

Strandness, D.E., Priest, R.E., and Gibbons, G.E. (1964). Combined Clinical and Pathologic Study of Diabetic and Nondiabetic Peripheral Arterial Disease. *Diabetes* 13**,** 366-372. doi: 10.2337/diab.13.4.366.

Sullivan, J.T., Grouper, S., Walker, M.T., Parrish, T.B., Mccarthy, R.J., and Wong, C.A. (2006). Lumbosacral cerebrospinal fluid volume in humans using three-dimensional magnetic resonance imaging. *Anesth Analg* 103**,** 1306-1310. doi: 10.1213/01.ane.0000240886.55044.47.

Sykova, E., Mazel, T., and Simonova, Z. (1998). Diffusion constraints and neuron-glia interaction during aging. *Exp Gerontol* 33**,** 837-851.

Takata, K., Matsuzaki, T., and Tajika, Y. (2004). Aquaporins: water channel proteins of the cell membrane. *Progress in Histochemistry and Cytochemistry* 39**,** 1-83. doi: http://dx.doi.org/10.1016/j.proghi.2004.03.001.

Turnbull, I.M. (1971). Microvasculature of the human spinal cord. *J Neurosurg* 35**,** 141-147. doi: 10.3171/jns.1971.35.2.0141.

Venero, J.L., Vizuete, M.L., Ilundáin, A.A., Machado, A., Echevarria, M., and Cano, J. (1999). Detailed localization of aquaporin-4 messenger RNA in the CNS: preferential expression in periventricular organs. *Neuroscience* 94**,** 239-250. doi: http://dx.doi.org/10.1016/S0306-4522(99)00182-7.

Verkman, A.S. (2009). Aquaporins: translating bench research to human disease. *J Exp Biol* 212**,** 1707-1715. doi: 10.1242/jeb.024125.

Virchow, R. (1851). Ueber die Erweiterung kleinerer Gefäfse. *Archiv für pathologische Anatomie und Physiologie und für klinische Medicin* 3**,** 427-462. doi: 10.1007/BF01960918.

Vitellaro-Zuccarello, L., Mazzetti, S., Bosisio, P., Monti, C., and De Biasi, S. (2005). Distribution of Aquaporin 4 in rodent spinal cord: relationship with astrocyte markers and chondroitin sulfate proteoglycans. *Glia* 51**,** 148-159. doi: 10.1002/glia.20196.

Wagshul, M., and Johnston, M. (2013). "The Brain and the Lymphatic System," in *Immunology of the Lymphatic System*, ed. L. Santambrogio. Springer New York), 143-164.
Waksman, G. (2006). *Proteomics and Protein-Protein Interactions: Biology, Chemistry, Bioinformatics, and Drug Design.* Springer.
Wang, D., and Owler, B.K. (2011). Expression of AQP1 and AQP4 in paediatric brain tumours. *J Clin Neurosci* 18**,** 122-127. doi: 10.1016/j.jocn.2010.07.115.
Wen, H., Nagelhus, E.A., Amiry-Moghaddam, M., Agre, P., Ottersen, O.P., and Nielsen, S. (1999). Ontogeny of water transport in rat brain: postnatal expression of the aquaporin-4 water channel. *European Journal of Neuroscience* 11**,** 935-945. doi: 10.1046/j.1460-9568.1999.00502.x.
Winkler, E.A., Bell, R.D., and Zlokovic, B.V. (2011). Central nervous system pericytes in health and disease. *Nat Neurosci* 14**,** 1398-1405.
Wisden, W., and Morris, B.J. (2002). *In Situ Hybridization Protocols for the Brain.* Academic Press.
Yang, L., Jones, N.R., Stoodley, M.A., Blumbergs, P.C., and Brown, C.J. (2001). Excitotoxic Model of Post-traumatic Syringomyelia in the Rat. *Spine* 26**,** 1842-1849.
Yasui, K., Hashizume, Y., Yoshida, M., Kameyama, T., and Sobue, G. (1999). Age-related morphologic changes of the central canal of the human spinal cord. *Acta Neuropathol* 97**,** 253-259.
Yaziji, H., and Barry, T. (2006). Diagnostic Immunohistochemistry: what can go wrong? *Adv Anat Pathol* 13**,** 238-246. doi: 10.1097/01.pap.0000213041.39070.2f.
You, H.J., Dahl Morch, C., Chen, J., and Arendt-Nielsen, L. (2003). Simultaneous recordings of wind-up of paired spinal dorsal horn nociceptive neuron and nociceptive flexion reflex in rats. *Brain Res* 960**,** 235-245.
Zelenina, M. (2010). Regulation of brain aquaporins. *Neurochemistry International* 57**,** 468-488. doi: http://dx.doi.org/10.1016/j.neuint.2010.03.022.

MACQUARIE UNIVERSITY

ANIMAL RESEARCH AUTHORITY (ARA)

AEC Reference No.: 2013/047-5 **Date of Expiry:** 2 January 2015

Full Approval Duration: *2 January 2014 to 31 December 2016 (36 Months)*

This ARA remains in force until the Date of Expiry (unless suspended, cancelled or surrendered) **and will only be renewed upon receipt of a satisfactory Progress Report before expiry *(see Approval email for submission details).***

Principal Investigator:
Dr Thomas Woodcock
School of Advanced Medicine
Macquarie University, NSW 2109
thomas.woodcock@mq.edu.au
0449 148 418

Principal Investigator:
Marcus Stoodley 0407 896 492

Associate Investigator:
Atieh Najafi 0435 148 822
Lucinda McRobb 0411 126 331

Research Assistant:
Xin Song 0423 492 959

Student:
Thomas Cusick 0400 217 141

In case of emergency, please contact:
the Principal Investigator / Associate Investigator named above
or Manager, CAF: 9850 7780 / 0428 861 163 and **Animal Welfare Officer**: 9850 7758 / 0439 497 383

The above-named are authorised by MACQUARIE UNIVERSITY ANIMAL ETHICS COMMITTEE to conduct the following research:

Title of the project: **CSF Physiology: Flow In The Spinal Cord And Subarachnoid Space**

Purpose: **4 - Research: Human or Animal Biology**

Aims: **To determine routes of fluid inflow and outflow from the CNS and how CSF flow obstructions in the subarachnoid space influence these flows and fluid homeostasis in the CNS.**

Surgical Procedures category: 5 - Major Surgery with Recovery

All procedures must be performed as per the AEC-approved protocol, unless stated otherwise by the AEC and/or AWO.

Maximum numbers approved (for the Full Approval Duration):

Species	Strain	Weight	Age/Sex	Total	Supplier/Source
02 - Rats	Sprague Dawley	~300g	~6 weeks Male	305	ARC Perth
02 - Rats	Sprague Dawley	any	~12 weeks Male	5	ARC Perth
			TOTAL	310	

Location of research:

Location	*Full street address*
Central Animal Facility	Building F9A, Research Park Drive, Macquarie University, NSW 2109
ASAM	Level 1, F10A, 2 Technology Place, Macquarie University, NSW 2109

Amendments approved by the AEC since initial approval:

1. ***Amendment #1*** *- Addition of 5 animals aged 12 weeks. (Exec approved 4 March 2014, ratified at the AEC 20 March 2014).*
2. ***Amendment #2*** *- Amend procedure / administration of substances. (Approved at the AEC meeting 17 July 2014).*
3. ***Amendment #3*** *– Addition of Lucinda McRobb as Associate Investigator. (Approved at the AEC meeting 14 August 2014).*

Conditions of Approval:

1. Dr Woodcock to be supervised for the first 20 times he attempts femoral vein catheterisation on live animals.

Being animal research carried out in accordance with the Code of Practice for a recognised research purpose and in connection with animals (other than exempt animals) that have been obtained from the holder of an animal suppliers licence.

Dr Karolyn White (Acting Chair, Animal Ethics Committee) **Approval Date: 14 August 2014**

Adapted from Form C (issued under part IV of the Animal Research Act, 1985)